Baja SAE Semi-Active Suspension

Final Design Review Report

March 15th, 2022

Project Members:

John DeBoer

deboer@calpoly.edu

Harrison Hirsch

hhirsch@calpoly.edu

Philip Pang

ppang@calpoly.edu

Stassa Cappos

scappos@calpoly.edu

Sponsor:

Professor John Fabijanic

Cal Poly Racing, Baja SAE

Mechanical Engineering Department

California Polytechnic State University,

San Luis Obispo

Abstract

This Final Design Review (FDR) Report outlines the senior design project of the Baja SAE Semi-Active Suspension group, which includes mechanical and electrical engineering students at California Polytechnic State University San Luis Obispo. This document compiles the Baja SAE Semi-Active Suspension senior project team's research and development of a semi-active suspension system for the Cal Poly Racing Baja SAE racecar. The goal is to design a system that adjusts the damping constant of the racecar's spring-damper suspension while the vehicle is being driven in order to improve vehicle dynamics and driver comfort. None of the semi-active dampers that exist on the market were built for a Baja SAE-type application. Initial technical and existing product research found that magnetorheological fluid, electrorheological fluid, and mechanical valving are the main three ways to vary damping rate in a given damper. Interviews with industry professionals and controlled convergence analysis of these damping adjustment methods lead the team to develop a concept design that focuses on adjusting high-speed compression damping using a mechanical actuator which is controlled by an electronic control loop. Further research and exposure to the off-road suspension industry encouraged the team to narrow the focus of the project to utilize an existing valve actuator and develop the control algorithm to retrofit the valve for the Baja application. The team's scope focused on developing an electronic interface and test bench setup to test the first iteration of the semi-active damper off-car. The team's results and recommendations for future projects are detailed in the results and conclusion sections respectively, and they serve as a starting point for the next senior project group that will continue the project's development for on-car applications.

Table of Contents

List of Figures

1. Introduction

The purpose of a vehicle's suspension system is to maintain the vehicle's kinetic energy by absorbing impacts from obstacles, modify oversteer and understeer capabilities, and reduce harsh accelerations felt by the driver. This is accomplished by creating a path for elastic load transfer through the suspension, and rather than inelastic load transfer through the chassis or other rigid components.

The Cal Poly Racing Baja SAE team builds a single-seater off-road racecar that traverses over a variety of rough terrain and obstacles during competition settings. The Baja SAE team currently utilizes traditional passive coilovers, which have manually adjustable compression and rebound damping rates, and they are looking for a way to intelligently and continuously vary these damping rates to improve ride quality for driver comfort and vehicle performance.

The purpose of this project is to develop a semi-active suspension system that integrates mechanical, electrical, and software control systems to automatically or semi-automatically adjust compression and rebound damping rates based on inputs from the varying terrain. The Baja SAE Semi-Active Suspension (SAS) senior project team aims to develop a semi-active suspension prototype for bench testing in 2022, and for use on the 2023 Cal Poly Racing Baja SAE racecar.

The Baja SAE SAS team consists of four team members, including John DeBoer (Electrical Engineering), Philip Pang (Mechanical Engineering, Mechatronics), Harrison Hirsch (Mechanical Engineering), and Stassa Cappos (Mechanical Engineering). This Final Design Report (FDR) presents the Baja SAE SAS team's background research on semi-active dampers, the project objectives, and a project management plan describing the projection of the project.

2. Background

2.1 Stakeholder/Need Research

When choosing passive damper rates for an off-road vehicle, often a compromise must be made to balance vehicle performance with driver comfort. Stiff suspension results in faster acceleration, braking, cornering, and reduces bottom-out and top-out events, while soft suspension can increase driver comfort and speed through highly technical situations [5]. Therefore, the best option for passive damping is to pick values somewhere in between that encompass both conditions. This results in a suspension system that handles sufficiently and is adequately comfortable for the driver but performs neither of those tasks exceptionally well. To mitigate this compromise, a system must be developed that can intuitively change the damping rate based on different driving conditions so that the operator does not need to stop the vehicle to manually adjust damping rates.

The first portion of design research was to identify the main stakeholders. The project is being designed to use on the Cal Poly Racing, Baja SAE racecar, which defaults the Baja team as the primary stakeholder. Interviews were conducted with professionals in the automotive suspension industry to give insight into the project needs.

2.2 Existing Solutions

When presented with the objective of changing damping rates, there are two main ways to achieve this: by changing the viscosity of the damping fluid or changing the internal valving geometry [7]. Current semi-active suspension products on the market use several methods of accomplishing this, like using magnetic or electric currents to change the properties of specialized fluids or using solenoids to change mechanical valving. However, these products exist mainly for on-road motorcycles and cars, and off-road full-size vehicles and UTVs. A solution does not yet exist for a small scale, Baja SAE sized application. A list of relevant patents is provided in Appendix A.

2.2.1 Adjustable Valve Damping

Perhaps the most intuitive solution to the variable damping problem is to physically change the internal valving of the damper. This method usually involves a solenoid that opens or closes orifices between the damper and external reservoir as it actuates. There are several examples of this method being used in production, such as Fox's Live Valve and iQS, Polaris's Dynamix damper system, and Can-Am's Smart Shox.

Manually adjustable dampers have compression and rebound knobs that offer a wide range of damping rates by physically moving an internal needle that opens or restricts fluid flow. A DC motor assembly can be fixed to these knobs to cycle through the different options, allowing for virtually infinite damping rates within the range of damping provided by the needle and orifice sizes.

In general, adjustable valving is the least complex and least expensive method [3]. However, the major drawback of this system is its reaction time. To accurately change damping to the correct value continuously, extremely quick reaction time is required, and this is limited by the mechanical speed of the valve actuators.

2.2.2 Magnetorheological and Electrorheological Fluid Damping

Magnetorheological (MR) and electrorheological (ER) fluid dampers effectively change the viscosity of the fluid to achieve different damping coefficients [9][12]. This works by exposing the fluid to a magnetic or electric field, which reversibly and instantaneously changes it from a free-flowing liquid to a semi-solid with controllable yield strength. The MagneRide system made by General Motors is the most common MR damper system on the market currently. The most apparent advantage to this method is the speed at which the system can react to an input. The reaction time for MR and ER dampers is significantly higher than that of an adjustable valve damper, making it much more viable in this regard [4]. However, this speed comes with a few hefty downsides. First, MR and ER fluids are extremely expensive. There are very few companies that produce these specialized fluids, and they can be in the range of $2000/liter. Second, the fluid itself is inherently abrasive and the particles will get stuck in corners and crevices, meaning it will have to be replaced and maintained frequently. Lastly, incorporating methods of activating these fluids, such as a custom electromagnet, will add a significant amount of weight to the system.

2.3 Technical Research

2.3.1 Hardware Control

Hardware controllers are used to achieve the fastest possible response times. For this project, a proportional integrating differentiating (PID) controller will be implemented. The proportional control will change the amount of damping within the system to ensure a desired damping coefficient is maintained most of the time. The integrating control will ensure the system reaches a desired steady-state value for the damping coefficient over long periods of time. Finally, the differentiating control will predict the immediate behavior of the system and react momentarily faster than the proportional control. Overall, a PID controller has been chosen because it can react quickly and can be used in any environment [7].

2.3.2 Software Control

Software control will be used in parallel with the PID hardware controller. Many semi-active suspension systems utilize what is known as a "skyhook" controller. This type of fuzzy logic controller has been developed specifically for semi-active suspensions and utilizes complex algorithms to control damping [13]. According to the graph below, the fuzzy "skyhook" software controller in tandem with a PID controller outperforms all other controller options [16].

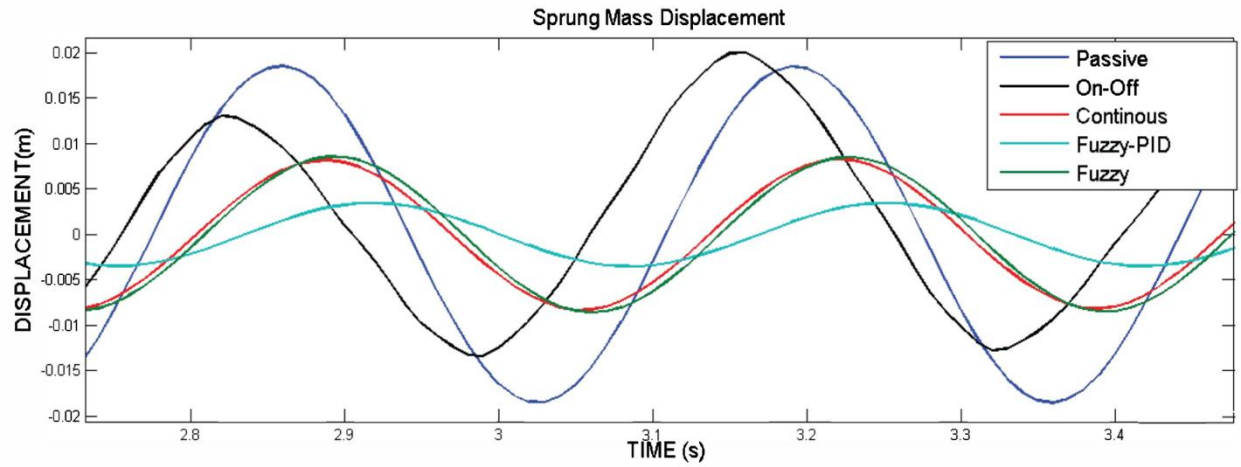

Figure 2.1 Displacement of dampers with various controllers over time, 3Hz [16]

In addition to the "skyhook" algorithm, the software controller will also handle user inputs to the system. This will allow the driver to easily interface with the system to manually control damping options.

2.3.3 Human Comfort

Research has been conducted regarding the comfort of humans throughout various environments. In an interview with Bobby Hodges, Program Manager at Nevada Automotive Test Center, the standards ISO 2631 and TOP 1-1-014 were discussed as a way to quantify a vehicle's ride quality. According to ISO 2631 [20], humans experience discomfort when experiencing frequencies 6Hz and above, and muscles begin to tense when frequencies above 10Hz are

encountered. Therefore, to maximize driver comfort, a semi-active suspension system must be tuned to act as a low pass filter with a corner frequency of 5Hz [18].

Additionally, research has been conducted regarding effective damping rates to mitigate driver discomfort. In an interview with Dylan Evans of Icon Vehicle Dynamics, it was said that increasing the damping rate of the system is almost always what makes the driver more comfortable. This is seemingly counter-intuitive but increasing the damping rate is the most effective means of preventing bottom-out, which causes the most driver discomfort. Therefore, the damping rate will be increased as the system detects rough terrain.

2.3.4 Hardware Design

The most common industry design currently utilizes a solenoid to control the flow rate of damper fluid between the main damper and the reservoir. The benefits of this design are its fast reaction times and its reliability. To explain, the reaction time of the system is about as fast as the solenoid takes to adjust. Dylan Evans of Icon Vehicle Dynamics stated that their dampers react in under 80ms, which is not a noticeable delay to the driver. Therefore, the Baja SAS shall react to terrain changes in under 100ms to remain competitive in the suspension market.

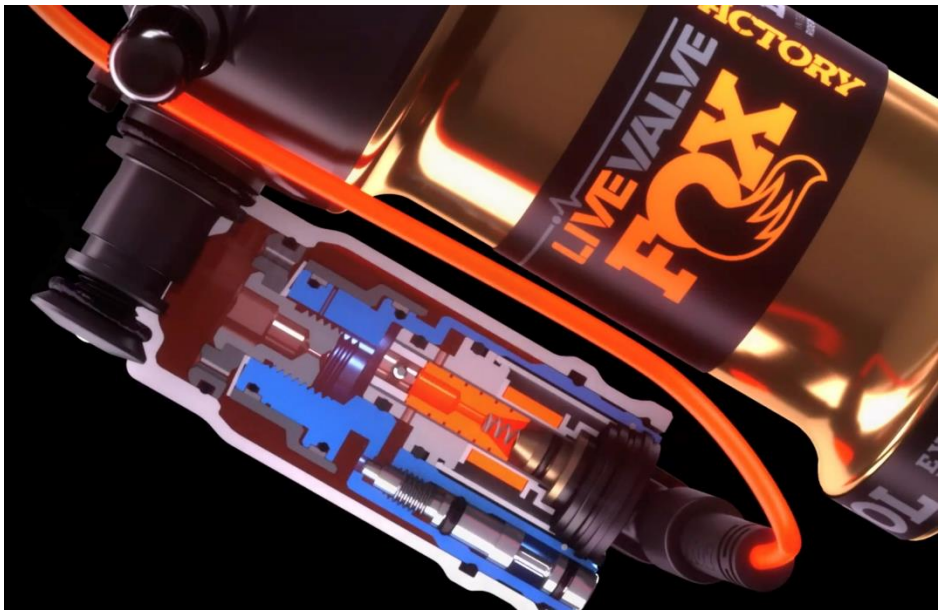

Figure 2.2 FOX Live Valve Solenoid [21]

Damon Pipenberg of Motivo Engineering stated in an interview that the damping adjustment knob found on the Baja car's current dampers could also be utilized to produce the same result as the solenoid design. The damping adjustment knob, found on the top of the Baja car's current passive dampers, could be redesigned to allow for stepper motor control. The benefits to this design would be the minimal modifications to the existing dampers (only the damping adjustment knob would need to be modified). However, there is uncertainty regarding the reliability of the existing internal valve adjustment mechanism, so this design would need to be tested early on for reliability.

2.3.5 Spring-Damper Adjustment Methods

There are five main adjustment methods to consider when tuning common spring-damper systems such as the passive coilover dampers on the Baja car. Firstly, the spring can be swapped out to achieve different spring rates or preload can be changed by lengthening or shortening the effective length of the spring while it is assembled on the passive coilover. Adjusting the spring affects ride height, roll center, and pitching when driving over obstacles. In this project, the spring rate and setup will remain constant as the vehicle operates and it will not be adjusted by the SAS system. The SAS will use the spring characteristics as inputs to the control system and the spring values can be updated in the control loop when the Baja team modifies the spring setup.

The additional four methods of adjustment focus on changing damper response characteristics, which includes high-speed and low-speed compression and rebound. Depending on the damper, all four characteristics can be changed by the user by rotating the compression and rebound adjustment knobs or by changing the internal valving shim stack. During an interview with Liam Mora, former Fox Factory Inc. Test Engineer Intern, it was established that about 80 to 90% of the damping occurs in the main damper chamber as fluid passes through the main piston's shim stack. Careful tuning of the shim stack can greatly improve vehicle performance. However, the damper must be fully disassembled to alter the shim stack, so it will be treated as a constant parameter for the SAS system. The remaining 10 to 20% of damping is controlled by the low and high-speed compression that occurs in the valving between the main damper body and the external reservoir. Additionally, the low-speed rebound can easily be adjusted with a knob on the damper body, but it was advised that the low-speed rebound does not need to be continuously altered because it is a function of unsprung mass and spring rate which are constant values. Therefore, the low-speed rebound can be manually set when based on the spring setup and unsprung mass characteristics.

Taking these factors into account, the SAS system will focus on adjusting two parameters: low and high-speed compression settings in the valving mechanism that controls fluid flow between the main body and external reservoir. The fluid has two possible flow paths depending on the rate of compression: through the low-speed orifice, which is affected by the placement of the low-speed adjustment needle, or through the shim stacks during high-speed compression. Low-speed compression is utilized to reduce effects of inertial forces such as the body rolling during cornering, or to dampen small disturbances such as chatter in the terrain that causes driver discomfort. High-speed compression occurs when the spring and damper compress quickly due to an impact such as a sharp obstacle or landing after a jump.

The Fox Dual Speed Compression (DSC) adjuster knob (Figure 2.3) allows for the adjustment of the low-speed and high-speed compression damping that occurs when fluid flows between the main piston and external reservoir.

Figure 2.3 Fox Dual Speed Compression Adjuster Knob

Rotating the low-speed knob moves the low-speed adjustment needle in or out to change the cross-sectional area of the orifice (Figure 2.4), which therefore affects the amount of damper fluid that can pass through. Adjusting the knob to be fully open retracts the needle and allows for the largest amount of fluid flow past the needle. Adjusting the knob to the fully closed position causes the needle to move inward and close off the orifice, therefore forcing all of the fluid to pass through the reservoir's shim stack.

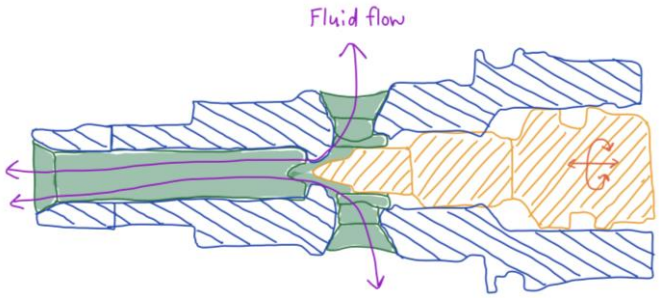

Figure 2.4 Low-Speed Compression Adjuster Cross Section

The high-speed compression can be adjusted by rotating the high-speed compression knob, which increases or decreases the preload of a spring that acts on the shim stack. Increasing the high-speed compression increases the preload acting on the shim stack which causes the shim stack to become stiffer. This causes more resistance, and the fluid must apply a higher pressure to pass through the shim stack into the external reservoir.

An important relationship to consider is that adjusting the low-speed compression circuit affects the transition to the high-speed compression circuit. By controlling the position of the low-speed needle, the fluid is either freely flowing through the low-speed orifice, or it is forced to flow through the high-speed shim stack. By altering low-speed compression, the flow through the shim stacks can be increased or reduced. However, adjusting the spring preload on the high-speed shim stack does not affect the low-speed damping circuit. This is because the fluid will always follow the path of least resistance, so if it the low-speed orifice is open it will flow

through past the needle before pressure causes fluid to pass through the high-speed shim stack.

3. Objectives

3.1 Problem Statement

Cal Poly Racing, Baja SAE needs a way to minimize driver fatigue and maximize performance at competition where their car encounters extreme road conditions such as 5 ft wall-drops, rock pits, and mud pits to name a few. Currently, since their manually adjusted suspension settings do not adjust during the race, the dampers are set at a compromise between handling and comfort.

3.2 Boundary Sketch

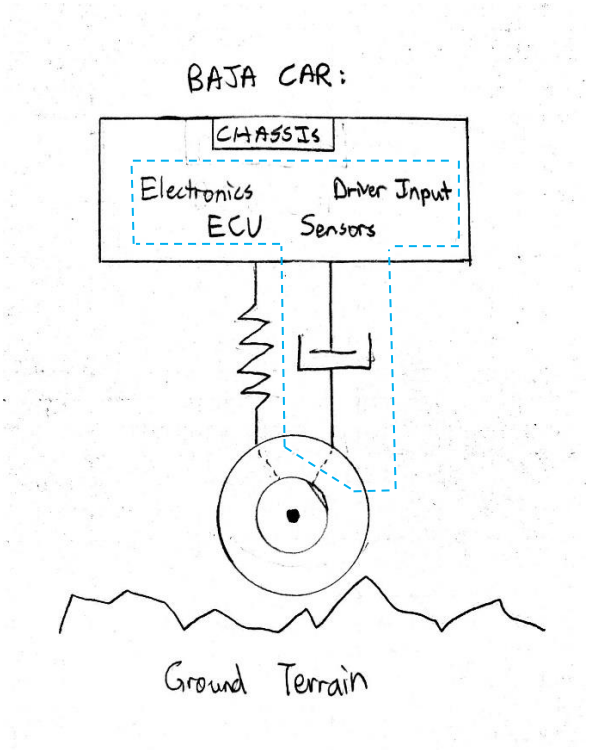

Figure 3.1 Boundary Sketch of SAS on Baja Car

The un-sprung mass accelerometers will be wired to the controller and the assemblies will receive power from the battery.

An accelerometer/gyroscope sensor will be placed under the driver's seat and driver controls will be located on the steering wheel for ease of access. These inputs will be wired to the controller and will receive power from the battery.

The controller will receive inputs from the accelerometers and gyroscope previously mentioned, and it will send output signals to the four damper assemblies. The controller will receive its power from the battery.

3.3 Stakeholder Needs/Wants

Table 3.1: Primary Stakeholder Needs/Wants

Needs	Wants
Fits on Baja car	Easy to produce
Variable damping ability	User tuning interface
Reaction time < 100ms	Easy to assemble
At least 8hrs before component failure	Drivable failure mode
Easily removeable	Low cost
	Weighs less than 30lbs

3.4 Quality Function Deployment

A quality function deployment process was used to verify the problem statement. A quality function deployment (QFD) house of quality chart is shown in Appendix B. The first goal of the QFD house of quality is to identify customers and customer needs/wants. Engineering specifications were quantities derived from customer needs/wants and are listed in the table below. Additionally, current products on the market were listed and ranked on the QFD house of quality to identify potential areas of improvement.

3.5 Engineering Specifications

3.5.1 Engineering Specifications Table

Table 3.2: Engineering Specifications Table

Spec. #	Parameter description	Requirement or target	Tolerance	Risk*	Compliance**
1	Reaction time	< 100ms	Min	H	A,T
2	Max weight	< 50lbs	Max	M	T
3	Cost	< $5000	Min	M	A
4	Damping options	9 tune settings	0/- 6	L	A,I
5	Frequency rejection	< 6Hz	Min	H	A,T
6	Damper length range	16–24in	Max	L	A,T
7	MTBF	> 8hrs	Max	H	T
8	Off-car assembly	< 60mins	Min	M	T
9	On-car assembly	< 20mins	Min	M	T

* Risk of meeting specification: (H) High, (M) Medium, (L) Low
** Compliance Methods: (A) Analysis, (I) Inspection, (S) Similar to Existing, (T) Test

3.5.2 Specification Justifications, Compliance Testing, and Risks

Reaction Time

Dylan Evans of Icon Vehicle Dynamics stated his industry-standard semi-active suspension system takes around 75ms to react. Significantly longer reaction times will not make the ride any smoother and can lead to control loop instability. Therefore, 100ms or less is a reasonable reaction time to verify the effectiveness of the system and compete with current industry products.

Reaction time can be tested and measured with simulation of the system in MATLAB's Single-Input Single-Output Tool (SISO Tool). Reaction time will be the defined as the time it takes for the system to reach 90% of its target value with a step response input. This specification has been labelled as high risk because it will require a well-tuned control loop and potentially expensive equipment (high-end motors or solenoids) to react fast enough.

Max Weight

The current passive coilovers have a net weight of about 24 pounds. A 50-pound max weight specification allows for the addition of heavier dampers and electronics components.

The net weight of the system will be defined as the total weight of all SAS components. This weight includes the dampers, controller, PCB, battery, and wires. The net weight can be measured by weighing the individual assemblies on a scale and adding their weights together.

Cost

The current passive coilovers cost around $2000, which requires the semi-active components of the system to cost below $3000 to reach the net goal of $5000. The electronics will add cost to the semi-active system, which includes integrated circuits, electronic proportioning valves, the microcontroller, the wiring harness, and the PCB manufacturing cost. Industry competitors, like Can-Am's Smart Shox, cost around $2000 with mass manufacturing. Therefore, to be competitive in the current market, a semi-active suspension prototype should not cost more than $5000 before mass production.

The cost of the system will be analyzed using a spreadsheet of receipt records.

Frequency Rejection

The aim of this specification is to utilize the dampers as a low pass filtering system to dampen frequencies 6Hz and above [20]. ISO 2631 [20] concludes that 6Hz is the frequency at which humans become very uncomfortable and quickly fatigued.

Frequency rejection will be analyzed using a MATLAB model of the car and will be physically measured with a gyroscope under the driver's seat. The measured roll and pitch waveforms of the vehicle will be plotted over time and used to verify frequencies of 6Hz rarely occur under typical operating environments. "Typical" will be defined as environments similar to the Baja SAE competition. Therefore, off-road trails in Pozo, CA will be used to test this specification, as they are similar to the Baja SAE terrain.

Mean Time Between Failures (MTBF)

The Baja SAE endurance competition lasts for 4 hours, and the Baja SAE team puts up to 8 hours of drive time on the car during a testing day. Therefore, 8 hours is a reasonable MTBF because it ensures the Baja car will last for the duration of the endurance race and testing days. The life cycle of the system requires that it last for at least 8 hours before encountering a component failure. Therefore, the battery will be tested to ensure it can store enough charge to supply the system for at least 8 hours. Additionally, all electronic housings will be tested up to and IP68 waterproof rating to ensure they do not fail due to environmental reasons. This has been labelled as a high-risk specification because the input environment is unknown and highly variable.

Off-car and On-car Assembly Times

The off-car assembly time is defined as the time it takes four SAS team engineers to assemble the SAS system away from the Baja car. A subjective survey of engineers concluded that 60 minutes or less is a reasonable time frame in which the system must be assembled off the car. Similarly, the on-car assembly time is defined as the time it takes four SAS team engineers to assemble the SAS system onto the Baja car. This time is shorter because the entire system may need to be replaced during the endurance race in the event of a failure. Therefore, 20 minutes is a reasonable time for the Baja car to be off the track before incurring a severe point loss. Off-car and on-car assembly times can be verified by timing the events with a clock.

4. Concept Design

The concept ideation and selection phase consisted of creating a functional decomposition Jamboard (figure 4.1), Pugh matrices (figures 4.11 - 4.13), morphological matrices (figure 4.14), and weighted decision matrices (figure 4.15). Ideation models and concept prototypes were created to test the functionality and feasibility of several ideas.

When beginning the concept design process, the three main areas of design development were the damping adjustment mechanism, the driver control input, and the electronic software and hardware control system. To develop a concept design, steps were taken to identify the primary and secondary functions of the system, and then these functions were broken down into the appropriate three categories. Then, Pugh matrices were utilized to evaluate different mechanisms and components to fulfill each function and the highest-ranking options were compiled into a morphological matrix, which was then used to compile several concept designs. Each concept design was evaluated based on its capabilities to meet the stakeholder's needs using a weighted decision matrix. This guided the design direction to converge on 2 concepts: using a DC motor or solenoid to adjust the low speed-compression needle based on inputs from the accelerometers and electronic control system. The following sections describe each stage of the concept design development that led to the concept design selection.

4.1 Ideation Process

The ideation process began by identifying specific functions that the semi-active suspension (SAS) system needs to perform. The stakeholder's primary needs (orange) are shown on the top of the functional decomposition diagram in figure 4.1. These needs were established in the QFD, and they incorporate specifications regarding system performance, packaging for implementation and durability, and maintaining driver comfort. To address these needs, secondary functions (yellow) and their attributes (green) were determined. The ideation process was recorded on a Google Jamboard (Figure 4.1).

Figure 4.1 Functional Decomposition

After the functions of the system were established, the team brainstormed different mechanical and electrical options to perform each function. These functions were explored through ideation models to iterate through different options to control damper valving and to provide driver input to the system.

Figures 4.2 to 4.6 represent options for assembly and packaging of electronically controlled valving, including the use of a solenoid or a DC motor to adjust the system's damping coefficient through internal valving. Creating these ideation models led to important discussions about the packaging of the electrical components. Namely, integrating the electronics in a way that ensures the safety and operation of the system amid harsh environmental conditions such as mud, water, and dust.

Figures 4.2 – 4.6 show ideation models testing variable damping functionality.

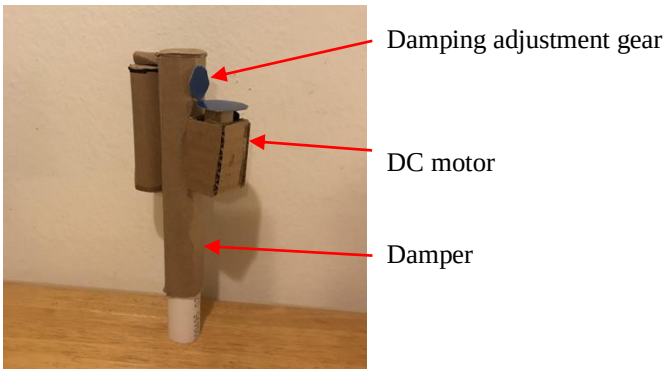

Figure 4.2 Damper Ideation Model 1

In the first damper ideation model, the damping coefficient is controlled by turning the damping adjustment gear with a DC motor. When the adjustment gear is turned, the internal valving changes such that the flow rate of damper fluid is varied between the damper body and its reservoir, which results in a change in the damping coefficient. This design opened the idea of a motor-controlled damping adjustment gear to our team. The benefits of this design are the ease of manufacturing and the serviceability. With this system, the motor can be swapped and adjusted without the need to decompress the damper fluid reservoir. However, there are a couple of downsides we discovered. The motor takes up a lot of space on the damper body, which leaves it susceptible to being knocked loose. Additionally, a custom damping adjustment gear assembly would need to be designed and manufactured to interface with the existing internal damper valving. This is one of the top design choices due to its simplicity, reliability, and cost effectiveness.

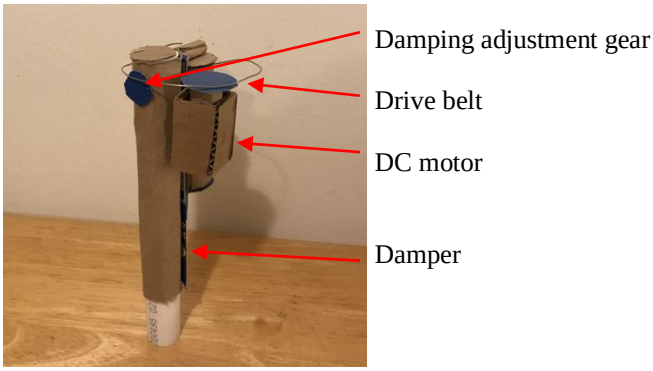

Figure 4.3 Damper Ideation Model 2

This design is like damper model 1, so it possesses the same pros and cons. However, the intention of this model was to enable the motor to be moved to the left or right of the damper case. This would mitigate the risk of knocking the stepper motor off the damper or breaking the motor altogether. However, the addition of a drive belt creates the risk of the belt breaking or running off its track, and a protective housing/track would require development to ensure the operation of this design. Therefore, the complexity and high failure rate of this design has ruled it out.

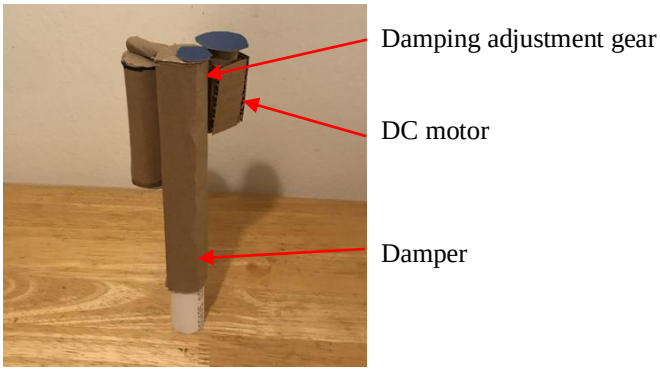

Figure 4.4: Damper Ideation Model 3

This model is like damper model 1, so it possesses the same pros and cons. However, the purpose of this design was to enable the motor to be positioned anywhere vertically and horizontally along the damper. This would ensure the motor could be placed in the safest possible location. The main change to this design is the damping adjustment gear, which has been moved to the top of the damper body. To allow this change, a damper must be purchased with the gear at this location. This could cause an issue if Baja SAE does not want to pay for new dampers. Therefore, this design has been ruled out because of its unnecessarily high cost.

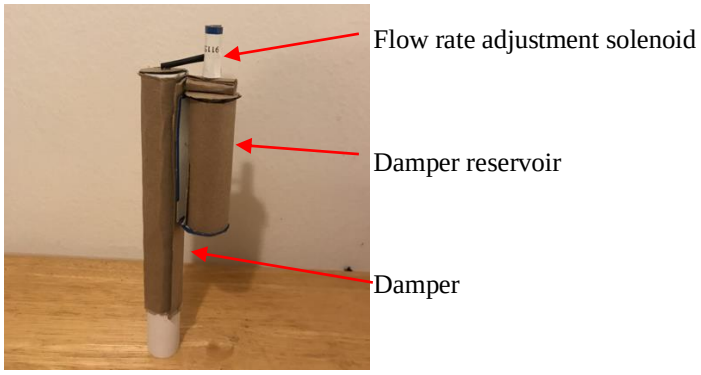

Figure 4.5 Damper Ideation Model 4

This model utilizes a solenoid and a damper fluid pipe to adjust the flow of damper fluid between reservoir and the main damper body. The main physical benefit to this design is the size, which is considerably smaller than the first 3 models. The solenoid can be placed in a safe position with little chance of encountering external forces. The downsides to this design include its difficulty to manufacture and difficulty to maintain. To explain, this design requires the existing passage between the main damper and the reservoir to be blocked and rerouted through a custom integrated pipe. Furthermore, any adjustment or hardware component swap would require the damper to be depressurized, and the fluid to potentially be replaced. However, the durability and reliability of this model is very high as this is the current leading industry design. Therefore, this is another top design choice for its reliability and compact packaging.

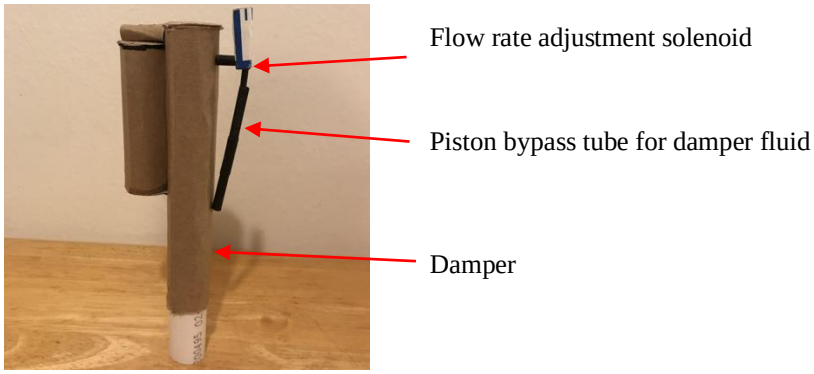

Figure 4.6 Damper Ideation Model 5

This design is like model 4, so it possesses most of the same pros and cons. The only difference is this is not an industry leading design. This model was created as a means of making manufacturing easier. The main damper body is the only part that needs to be tampered with, while the reservoir may be left alone. This design uses a solenoid to control the flow of damper fluid from the top and bottom of the damper (both sides of the piston). This enables the piston to be bypassed to decrease the rebound of the damper. The main drawback to this design is the susceptibility of the pipes and solenoid to outside forces. Additionally, this design only allows for the rebound to be adjusted – not the damping – so this design has been ruled out.

Additionally, driver controls were explored in Figures 4.7 - 4.10. These models considered the function of the driver controls and the placement of the buttons, knobs, and switches on the

steering wheel to provide the driver ease of access to the mechanism. Ergonomics is most important if the vehicle is traversing through rough terrain because the driver must maintain their hand placement on the steering wheel, so the mechanism must be easy to reach and activate.

Figure 4.7 Driver Controls, Override System Flip Switch I/O

Figure 4.8 Driver Controls, Togglable I/O Button

Figure 4.9 Driver Controls, Slider Switch

Figure 4.10 Driver Controls, Push-Hold I/O Button

To conclude the results from the ideation models above, the leading driver controls design is the togglable I/O button. This design has been chosen because it requires the least amount of time for the driver to spend with their hand off the wheel, and it is the least likely design to encounter unwanted inputs (e.g. Accidentally flipping a switch).

4.2 Ideation Refinement

After performing functional decomposition, brainstorming, and constructing ideation models, the next step was to objectively evaluate the options for each aspect of the semi-active suspension system. To do this, Pugh, morphological, and weighted decision matrices were utilized to compare possible valving mechanism and driver control options.

4.2.1 Pugh Matrices

Pugh matrices were used to analyze the mechanical aspects of the semi-active suspension system, specifically the damping adjustment and driver controls. Each Pugh matrix had a concept that acted as a datum, and the other options were compared to the datum for each function. A +, –, or S was used to indicate if a component performed a function better, worse, or the same as the datum. These symbols equaled +1, -1, or 0 respectively and each component received a total score to rank it in comparison to the datum.

At the start of the project, two methods of damping adjustment were considered: changing the viscosity of the fluid or changing the mechanical valving. These options are evaluated in Figure 4.11.

		Concepts					
		Knob Adjustment on Passive Coilover	Fully-Active Suspension	MR Semi-Active Suspension	ER Semi-Active Suspension	Solenoid-Valve Semi-Active Suspension	Passive Coilover
Criteria	Low Cost	0	-1	-1	-1	-1	1
	Durability/Life-Cycle	0	-1	-1	-1	1	0
	Response Time	0	1	1	1	1	-1
	Packaging/Size	0	-1	1	1	0	0
	Lightweight	0	-1	0	0	0	0
	Low Maintenance	0	-1	-1	-1	0	0
	Safe/driveable Failure Mode	0	-1	-1	-1	-1	0
	Damping Variability	0	1	1	1	1	-1
	TOTAL:	DATUM	-4	-1	-1	1	-1

Figure 4.11 Damping Adjustment Pugh Matrix

The result of Figure 4.11 indicates that adjusting mechanical valving with a solenoid in the reservoir or by adjusting the compression knob directly with a motor ranked as the highest options. Due to their complexity, expense, and difficulty of implementation the magnetorheological (MR) and electrorheological (ER) fluid adjustment options ranked poorly, while the manual hand adjustment of the passive coilover compression knobs ranked in the middle of the field. Although fluid control has extremely quick reaction times, this method was dismissed completely after multiple interviews with engineering professionals. This is due to the consideration of expense and difficulty to handle during assembly, as well as complications brought about by having small particles suspended in a fluid exposed to high shear loads. A main concern with using MR or ER fluids is that the particulates that allow for viscosity changes in the fluid might get stuck in crevices in the damper chamber and cause undesirable fluid viscosity distribution. This also means the fluid obtains abrasive properties, causing undesirable wear within the damper internals. These factors, combined with the extremely high cost of variable

viscosity fluids, make this option less feasible, as regularly servicing a semi-active suspension system is not in anyone's best interest.
Due to this large development in damping adjustment, new Pugh matrices were constructed to further analyze options for mechanical valving options. Additionally, upon further consideration of the implementation of control loops to adjust both high and low speed compression and rebound, it was decided that the most effective approach is to focus on adjusting compression characteristics, specifically the low-speed compression valving. This was discussed in further detail in the background, but it is an important design consideration for the mechanical valving concept selection because choosing to only control low-speed compression as compared to low and high-speed compression and rebound significantly reduces the amount of control loops that must be implemented. Concepts were selected that performed adjustments specifically to the low-speed compression valving and they were compared in Figure 4.12.

		Concepts					
		Latching Solenoid	Motor on Needle	Motor on Existing Knob	Off-the-shelf Linear Actuator	Motor on Worm Gear	Motor/Gearbox/Needle
Criteria	Low Cost	0	1	1	0	-1	1
	Durability/Life-Cycle	0	1	1	0	-1	0
	Complexity	0	1	0	1	-1	-1
	# of Distinct Damping Settings	0	1	1	1	1	1
	Safe/Drivable Adjustment Failure Mode	0	-1	0	0	-1	0
	Packaging/Size	0	0	-1	-1	-1	0
	Control Loop Simplicity	0	0	0	1	0	1
	Power Consumption	0	0	1	0	1	0
	Response Time	0	-1	-1	-1	-1	-1
	TOTAL:	DATUM	2	2	1	-4	1

Figure 4.12 Damping Adjustment, Valving Specific Pugh Matrix

After comparing six methods of changing the mechanical valving, the highest-ranking options centered on a method of adjusting the position of the low-speed compression needle by using a motor with a gearbox or lead screw or a solenoid to adjust because this offers a less complex method of making fine tuning adjustments to the low-speed compression. Adjusting the compression knobs was also highly ranked for its low cost and high durability.
When considering options for driver controls, consideration was given to the ergonomics, durability of the input mechanism, expense, and ease of integration as seen in Figure 4.13.

		Concepts						
		Push I/O Button	Rocker Switch	Push-hold Button	Clicker Knob	Flip Switch	Slider Switch I/O	Slider Switch (3-Settings)
Criteria	Ease of Use	0	-1	-1	-1	-1	-1	-1
	Low Cost	0	1	1	-1	1	1	1
	Ease of Assembly	0	0	0	-1	0	0	-1
	Ergonomics	0	-1	0	-1	1	1	1
	Ease of Diassembly	0	0	0	-1	0	0	-1
	Adjustment Variability	0	0	0	1	0	0	1
	Weather Proof	0	-1	0	0	0	-1	-1
	Visual Feedback (LED)	0	0	-1	-1	-1	-1	-1
	TOTAL:	DATUM	-2	-1	-5	0	-1	-2

Figure 4.13 Pugh Matrix Analyzing Driver Interface

For driver controls the option that ranked the highest was the flip-switch option. At first this was surprising, since the other options offered more variability and more advanced characteristics. However, in reviewing how the flip-switch ranked compared to the datum, it seems that simplicity came out as more important than user selectable settings. Similarly ranked was the push-hold button and the on/off slider switch. These options also offered the on-off simplicity, and it was logical that cutting out the option of multiple positions would be more beneficial for a driver who is focusing on racing and does not have the time or ability to focus on selecting a certain setting.

After constructing the Pugh matrices to evaluate different concepts for mechanical valving and driver controls, the various components were compiled into a morphological matrix to create various concept design combinations.

4.2.2 Morphological Matrix

In the following morphological matrix, different solutions and ideas that satisfy every function of the final product and objective are combined to make four distinct concepts to be compared in the next section in a weighted decision matrix. Here, one idea from each column is selected to make unique combinations. These unique combinations are described below Table 4.1.

Table 4.1 Morphological Matrix

Morphological Matrix				
Function	**Idea 1**	**Idea 2**	**Idea 3**	**Idea 4**
Adjustment Method	Motor on Knob	Motor on Lead Screw	Latching Solenoid	Linear Actuator
Button Type	Push/Hold	Push/Push	Flip Switch	Slider
Control Input Type	Manual	Sensor: Accelerometer	Sensor: Pressure Tap	Sensor: Linear Potentiometer
Damping Range Type	Low Speed Compression	Low-speed compression	Low-Speed Rebound	

Four concepts were created to incorporate features that satisfy each function. The concept designs are described in detail as follows:

Concept #1:

Damper is adjusted by motor directly connected to needle which is adjusting low-speed compression, taking instructions from manual input from driver using push/push buttons as well as control system taking sensor input from accelerometer measuring damper travel speed.

Concept #2:

Damper is adjusted by motor fitted onto existing knob which is adjusting low-speed compression, taking instructions from manual input from driver using push/push buttons.

Concept #3:

Damper is adjusted by latching solenoid which is adjusting low-speed compression, taking instructions from control system taking sensor input from accelerometer measuring damper travel speed.

Concept #4:

Damper is adjusted by motor connected to knob, which is adjusting high-speed compression, taking instructions from manual input from driver using push/push buttons as well as control system taking sensor input from accelerometer measuring damper travel speed.

It was challenging to combine the different solution ideas in a non-arbitrary manner because they seem so independent of each other. The main pattern that was used when it comes to different adjustment strategies (analyzed in Figure 4.12), was how the amount of time it takes to make adjustments help define whether to use manual controls only due to how quickly adjustments could be made.

For example, in Concept #2, with a motor fit onto a knob with detents, the number of distinct damping settings is limited to around ten settings. This knob would take longer to adjust due to the detents and thus, would likely be ineffective in adjusting due to constant, rapid sensor inputs. (Simulations will need to be done to show this.) In Concept #3, the latching solenoid adjusts very

quickly even though it only has two distinct settings, open and closed. Thus, it seemed logical to give such an actuator rapid, constant sensor input while it would not make a very big difference if biases were implemented from the driver's manual input. In Concept #4, high-speed compression was considered to see how it stacked up against Concept #1, which was a combination of all the highest ranked solution ideas for each column (function).

4.2.3 Weighted Decision Matrix

The four design combinations described above that were formed from the morphological matrix are then investigated in a weighted decision matrix.

CRITERIA	Weight:	Concept 1		Concept 2		Concept 3		Concept 4	
	1-5	Score	Total	Score	Total	Score	Total	Score	Total
Packaging	4	4	16	3	12	2	8	3	12
Response time	5	3	15	0	0	5	25	2	10
Usability	5	3	15	2	10	5	25	3	15
Number of distinct damping rates	2	4	8	3	6	1	2	3	6
Damping range	4	4	16	4	16	3	12	2	8
Durable valving and internals	4	3	12	3	12	5	20	3	12
Manufacturability	4	4	16	5	20	2	8	5	20
Serviceability	3	4	12	5	15	3	9	5	15
Cost	2	3	6	5	10	3	6	3	6
Lightweight	1	3	3	3	3	3	3	3	3
	TOTAL	119		104		118		107	

Figure 4.14 Weighted Decision Matrix

In this weighted decision matrix, each concept is stacked against each other according to the criteria listed on the left. These criteria are assigned weights to account for how some criteria are more important than others. The weights that were given here are from 1-5. Each concept was then scored in each criterion from 1-5. After each criterion score is multiplied by the respective weight, the weighted scores are totaled up in the bottom to compare to the different concepts. Starting with the lowest scoring concept, Concept #2 was created to analyze a system that is only controlled manually. With less options and no sensor input, the comfortability of this system would be lacking as adjustments will only be made between driving modes and different terrains. The usability of this system would be low as the performance of such a system is solely dependent on the driver.

Concept #4 was included in the decision matrix to see how adjusting high-speed compression instead of low-speed compression would affect the decision. Adjusting high-speed compression is essentially adjusting preload on the spring that is preloading the shim stack in the path from the main piston to the external reservoir. The only thing this does is adjust the threshold between high and low speed damper travel. With this design, its score for damping range really suffered. It does not necessarily change the damping rates for any range of damping forces. It merely changes when high-speed compression characteristics are used instead of low-speed compression rates. In fact, low-speed compression adjustments affect high-speed compression threshold but not the other way around. In addition, because low-speed damper travel is where the Baja SAE car will spend the most time, that is ultimately where adjustments will make the biggest difference.

Concept #1 scored the best, but only by a narrow margin to Concept #3. These two concepts are very strong in very critical but different aspects: manufacturability and response time. The team has learned that a solenoid actuated system would be able to adjust quicker than a motor system where numerous mechanical components would flex when given an input, delaying the demanded response. In this application, milliseconds matter. How critical of a difference in time response between these two concepts has yet to be calculated and/or tested. This is especially hard to judge, especially because the motor, gearbox, and solenoid have not been specified so no direct comparison can be made just yet. The next aspect to consider between Concepts #1 and #3 is manufacturability.

Compared with the rest of the concepts which all use motors to move the needle, the solenoid in Concept #3 is anticipated to be extremely hard to implement. The needle would need to be redesigned because its external threads would not be used and would interfere with the linear motion of the solenoid. Obviously, without threads, the mechanism would need to be sealed in a different way, which will require thorough testing. Lastly, because Concept #3 a solenoid, there really are only two main positions, open and closed. At this point in the team's research, it is not known whether or not these two main positions are enough. The team plans to investigate this further as well.

In conclusion, if a motor-actuated system is found to be fast enough to be adjusted effectively and continuously, it will be the best choice in terms of manufacturing and simplicity. If not, however, the solenoid solution will be pursued despite the anticipated complexity of its implementation.

4.3 Final Concept Design

The two final designs focus on adjusting low-speed compression by moving the low-speed needle in the external reservoir. The needle position will be controlled by an electronic control loop, which takes inputs from the accelerometers on the unsprung and sprung masses. From there it determines the most appropriate damping constant for the situation, and then outputs the corresponding needle position. There are two actuation options for moving the needle: using an electric solenoid in-line with the needle, or a DC motor and gearbox setup.

4.3.1 Needle Actuation Type

The first option utilizes a DC stepper motor to position the needle in a specific location, from closed to open and any position in between. The concept design in Figure 4.16 illustrates the stepper motor directly connected to the low-speed needle using a lead screw. As the motor spins, the needle extends or retracts into the low-speed damping orifice, effectively changing the damping coefficient.

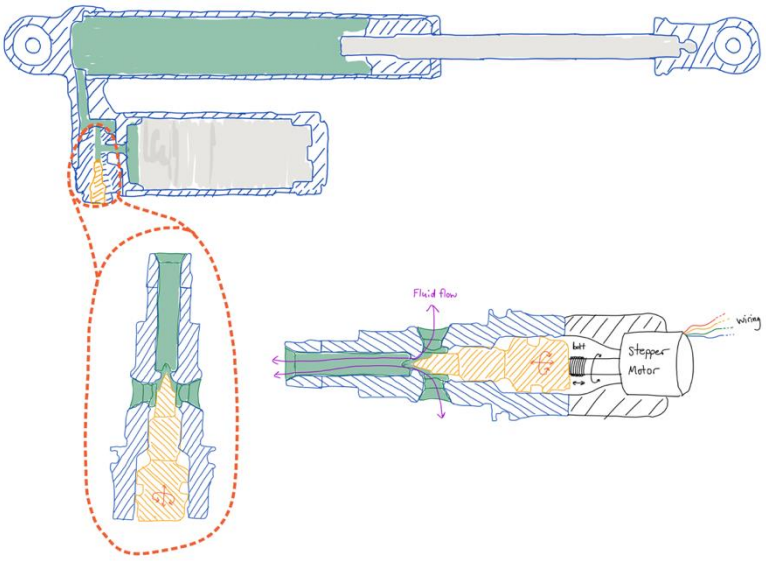

Figure 4.16 Variable Damping Mechanical Concept Design

The DC stepper motor can also be positioned in parallel to the needle in order to improve packing options. This option is illustrated in the concept CAD in Figure 4.17. To move the needle, the gear on the output shaft of the motor meshes with a gear that rotates a lead screw which in turn translates the needle in or out of the assembly. The gear ratio can be selected to increase speed or torque depending on the requirements of the system.

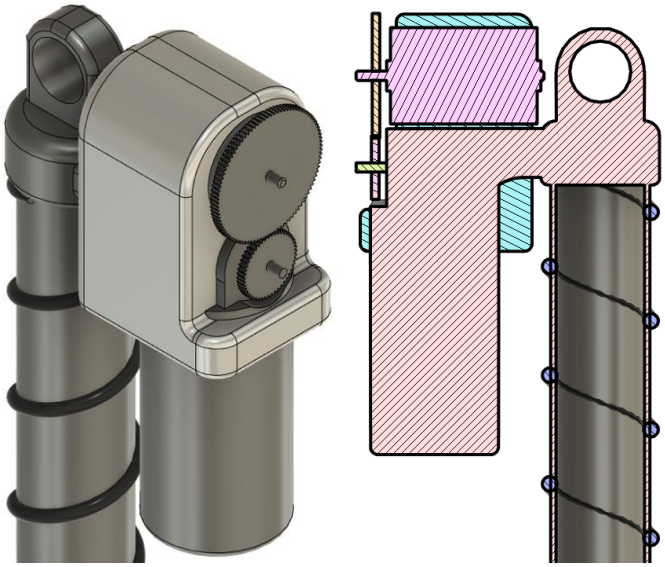

Figure 4.17 DC Motor Actuator with Gearbox CAD

Both orientations of the DC stepper motor provide a spectrum of infinite low-speed needle positions between the fully open and fully closed needle positions. This correlates to an infinite range of damping coefficients within these bounds, which is advantageous for choosing the most effective damping coefficient for each driving situation. However, this design incorporates multiple moving parts, which increases the opportunity for component failures as well as

mechanical losses. Additionally, the low-speed needle adjustment speed may be limited by the reaction time of the mechanisms.
Because of these concerns, a second design concept that utilizes an electric solenoid is also being considered for its mechanical simplicity and reaction time. This concept uses a linear solenoid to extend and retract the low-speed compression needle between two positions, and it is illustrated in Figure 4.18. The control loop will continuously adjust the needle to be in the fully open or fully closed position based on input from the vehicle sensors.

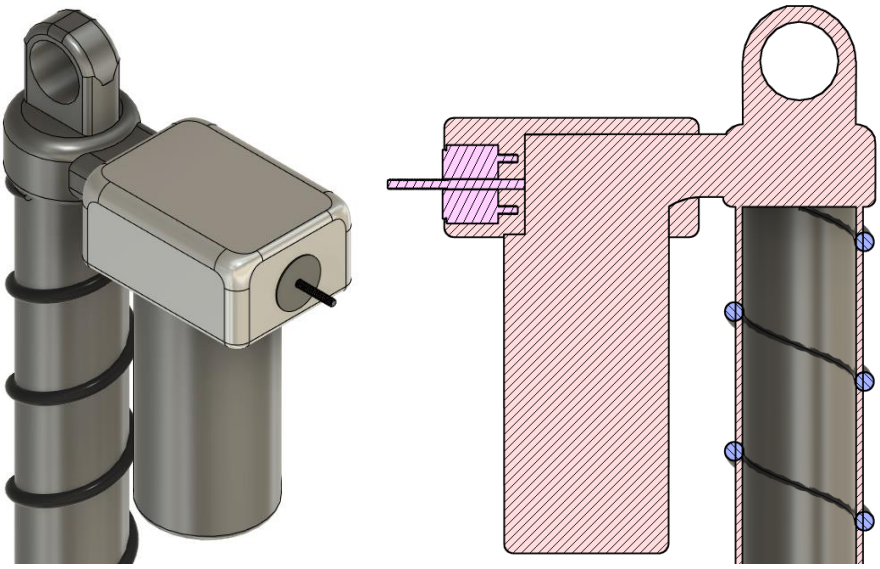

Figure 4.18 Solenoid Actuator CAD

The benefits of this system are its fast low-speed needle adjustment speed, compact design, and mechanical simplicity. There is only one moving part to this system, which will reduce the frequency of malfunctions. While the electric solenoid offers quicker response times because it is directly connected to the low-speed needle, it is limited in needle position options because the solenoid only provides two orientations: fully extended or fully retracted. In order to address this characteristic, complex controls software must be developed for this design to compensate for the two solenoid positions by utilizing a duty cycle to vary damping.

However, a high-end solenoid is required for this design, which significantly increases the cost. Additionally, testing will be required to determine the output force of the solenoid and its compatibility with a low-speed needle. The results of this testing could void its mechanical feasibility if the solenoid cannot output sufficient force. Additionally, there is a chance this design could become mechanically complex if the low-speed needle needs to be redesigned to make it mechanically compatible with the solenoid.

4.3.2 Electronic Control Loop

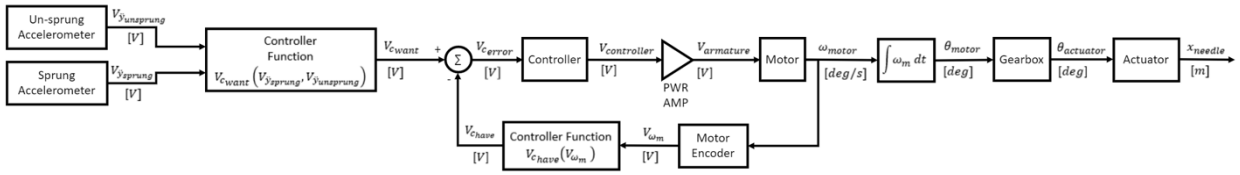

Figure 4.19 System Control Loop

The control loop shown above has been developed for the top damping adjustment design, with the omission of driver controls. As discussed in sections 2.3.1 and 2.3.2, the overall controller will consist of a software control algorithm and a hardware PID controller.

The purpose of this control loop is to reduce the vertical acceleration of the sprung mass, which is achieved by continuously applying the ideal damping coefficient to the system. Based on the acceleration, velocity, and position of the sprung and un-sprung masses, the following controller function has been derived to output the ideal damping coefficient:

$$c_{want} = \frac{\ddot{y}_{sprung} m_{sprung} + k_{damper}\left(y_{sprung} - y_{unsprung}\right)}{\dot{y}_{unsprung} - \dot{y}_{sprung}}$$

The velocity of the sprung and un-sprung masses will be measured by integrating accelerometer inputs. Accelerometers have been chosen due to their small size, low cost, and durability. The next best sensor option is to use linear potentiometers on the sprung masses to determine their velocities. However, linear potentiometers are large, fragile, and difficult to integrate.
The position of the low-speed needle will be measured through a motor encoder. As seen on the right side of the control loop, the position of the low-speed needle can be determined from the position of the motor shaft through a few simple conversions. The low-speed needle position can be converted to a damping coefficient using dynamometer testing data. Damping coefficient data will be recorded for at least 10 different low-speed needle positions, and the controller will utilize a look up table (LUT) to determine the closest damping coefficient to real-time encoder data.

The low-voltage controller output will be sent through a power amplifier with a 12V output and sufficient current sourcing capabilities. The power amplifier will be specified after the motor is chosen to determine current sourcing requirements. The motor, gearbox, and actuator will be used to control the flow of damping fluid between the main damper and its reservoir by adjusting the linear position of the low-speed needle (as pictured in figure 4.20). This will adjust the damping coefficient, giving the system variable damping capabilities.

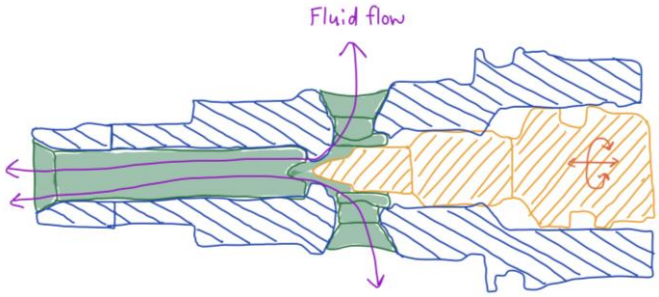

Figure 4.20 Low-speed Needle (Orange) and Damping Fluid (Purple)

4.4 Preliminary Design Risks

Before any manufacturing or testing can be done, necessary precautions must be taken to ensure the safety of anyone manufacturing, testing, or operating the semi-active suspension system. The Design Hazard Checklist in Appendix D indicates that the system may be unsafe due to the high accelerations that can occur inside the damper, as well as a large amount of energy being stored in the springs. While these are potentially dangerous aspects of any design, there are several reasons the severity of them may be lessened for this particular design project.
Regarding high accelerations being transferred from the road into the suspension, one of the main purposes of any vehicle's suspension system is to damp out these accelerations. Therefore, any high acceleration capable of causing harm is happening where the tire touches the road, and due to the way dampers are designed, that energy associated with these high accelerations will be dissipated before it can be resolved through the chassis, potentially injuring the driver or breaking components.

Another source of high accelerations could be from the adjustment needle. If enough pressure is generated inside the damper, the fluid could force the needle back out of the housing at high speeds, potentially endangering the driver. To prevent this, the housing for our selected method of needle adjustment will be made with a cover to block the needle if it is ejected, and the external piggyback reservoir will be pointed away from the driver.

In regard to energy being stored in the springs, none of it will be released into the driver in a hazardous manner. This is because coilovers are designed with viscous dampers, who's main purpose is to dissipate the energy from the road stored in the springs in a controlled manner.
In conclusion, while the environment that a semi-active suspension system is meant to operate in brings with it some potential safety concerns due to high amounts of energy being transferred and stored throughout the system, many of them can be disregarded since the purpose of the dampers in a vehicle's suspension is to safely dissipate this incoming energy. For any direct threats to the safety of the driver, the housings will be designed to shield the driver and the dampers will be positioned far enough away and oriented in such a way that any hazardous release of energy will not affect the driver.

5. Final Design

This section discusses the final design, its functionality, all safety, maintenance, and repair considerations, and the prototype cost analysis.

Since developing the final concept design, further research into the application and development of a custom valving device in parallel with a Baja-specific damping control loop appeared out of scope for this project. After discussions with Test Engineers at Fox Factory, the team decided to narrow the scope of the semi-active suspension project to focus primarily on the development of the electrical and software aspect of the control system. The semi-active system will utilize a Fox Live Valve and Fox damper paired with the hardware and software developed by the senior project team. The focus of the current team is to develop the control algorithm and hardware to retrofit the Fox setup to work for the Baja SAE application. After the Baja control system is established, it is recommended that future teams can continue the project by designing a custom valve adjuster that fits the Baja team's current dampers.

5.1 Mechanical Functionality

The mechanical system will utilize a 2.5-inch body, 5/8-inch shaft Fox damper paired with an electronic proportioning valve that will restrict flow in the base valve to make damping adjustments (Figure 5.1). These components were provided to the project by Fox Factory.

Figure 5.1 2.5" OD x 7/8" Shaft Fox Damper & Fox Live Valve Adjuster

At this time, the proportioning valve requires a damper with 7/8-inch shaft due to fluid flow requirements. There is no Live Valve or equivalent valve adjustment mechanism method that is compatible with the Baja team's mini UTV dampers, which have a 5/8-inch shaft. The damper we chose was selected because it has the correct size shaft to be compatible with the Fox Live Valve component, and has enough bleed to provide an appropriate damping range for a lightweight vehicle such as the Baja car. However, the damper is intended for a traditional off-

road UTV (utility terrain vehicle), and it is physically too large for the Baja SAE application, which is a mini off-road UTV. Therefore, the damper will be modified to fit the Baja application as discussed later in Chapter 6 (Manufacturing Plan).

Figure 5.2 Prototype Semi-Active Damper (left) & Current Passive Damper (right)

The larger damper will be used in the rear suspension only due to packaging constraints in the front suspension. This damper has an 8" stroke length, so it will provide the necessary amount of travel to meet the Baja car's 8" suspension travel requirement. However, this setup is not intended for competition use due to the added weight and size and lack of compatibility in the front suspension. This setup will be the first prototype of the custom Live Valve application, and it is intended to equip future projects with the technology for use with future custom valve adjustment mechanisms.

The Fox Live Valve operates similarly to the proposed custom valve adjustment design; a solenoid is used to move the base valve damping adjustment needle in relation to the base valve orifice. The needle position is adjusted by sending current to the Live Valve, which causes the needle to extend or retract. The needle will be controlled by the microcontroller which features the custom control algorithm, which is discussed in Section 5.2.

The control algorithm will determine the desired valve position by evaluating real-time vehicle data and comparing the data to known damping curves that were obtained through testing. The data will be collected with a rotary potentiometer on each of the Baja car's A-arms. The data will then be extrapolated to determine damper extension and compression position and velocity.

The prototype rotary potentiometer mounts will be 3D printed to allow for ease of assembly and design iteration. Additionally, 3D printing is a lightweight option and it can be manufactured using on-campus resources (discussed further in Chapter 6).

If the electronic system fails, the needle will move to the default position of fully extended, which closes the high-speed valve and results in a stiff damper. Since the focus of the system is to prevent bottom-out of the damper, it is more advantageous to drive with the valves fully closed than fully open. When the valves are fully closed, the ride will be less comfortable for the driver over low-speed chatter and bumps, but the vehicle will not bottom-out on in extreme cases, such as impacting large obstacles or when landing after a jump or drop. Therefore, the specification for a drivable failure mode is met.

5.2 Electrical Functionality

5.2.1 Hardware

The overall function of the electronics system is to adjust the damper valve current as a function of damper position. As the damper valve current changes, the force vs. velocity curve for the damper changes, making the damper harder/softer.

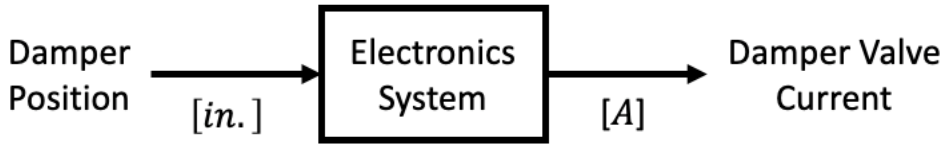

Figure 5.4 Electronics Hardware Overall Black Box Diagram

The design utilizes a PID controller to continuously predict the ideal output current as a function of damper movement. As seen in the diagram below, the damper position is measured as a voltage with a potentiometer. The velocity and acceleration signals are calculated using operational amplifiers.

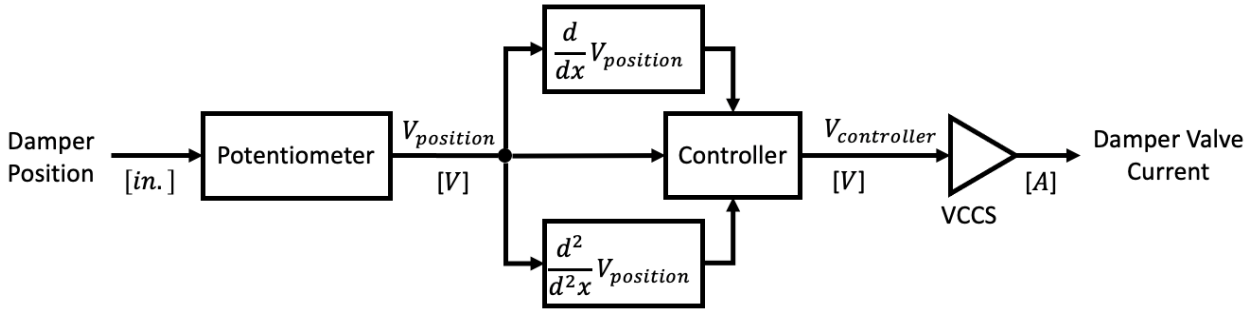

Figure 5.5 Electronics Hardware Expanded Black Box Diagram

5.2.1.1 Electronics Schematic

The entire electronics system has been realized as the schematic shown below. The system is powered by a single 12V battery. A 12V-to-3.3V voltage regulator is used to supply a 3.3V line to the controller and peripherals. The controller utilizes the data from the potentiometers to determine the appropriate output voltage for each of the dampers. The control algorithm is discussed later in the electronics software section, and the damper control circuit is discussed later in the electronics hardware section.

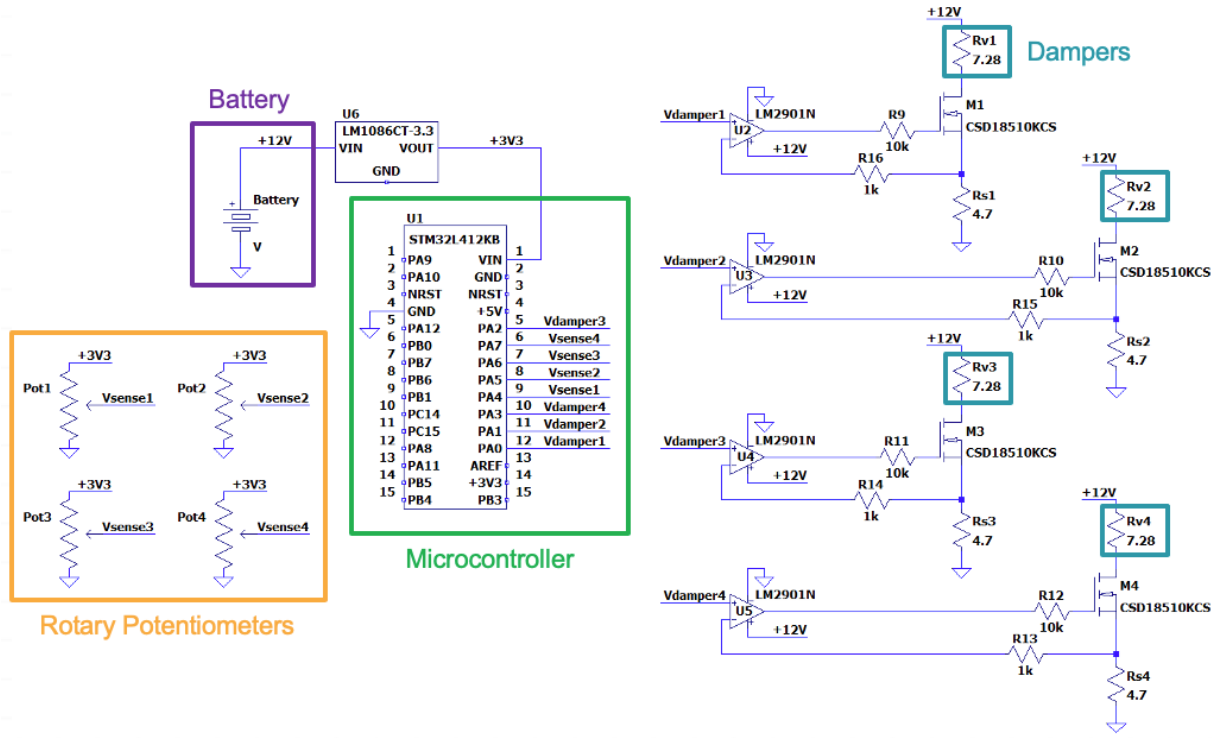

Figure 5.6 Electronics Overall Schematic

5.2.1.2 Electronics CAD

The figures below display the electronics assembly. The left figure displays the bare PCB, and the right figure displays the PCB with the microcontroller and headers, the electronics enclosure, and the connector assemblies. Molex brand connectors allow the PCB assembly to easily connect/disconnect from the wiring harness during the test phase.

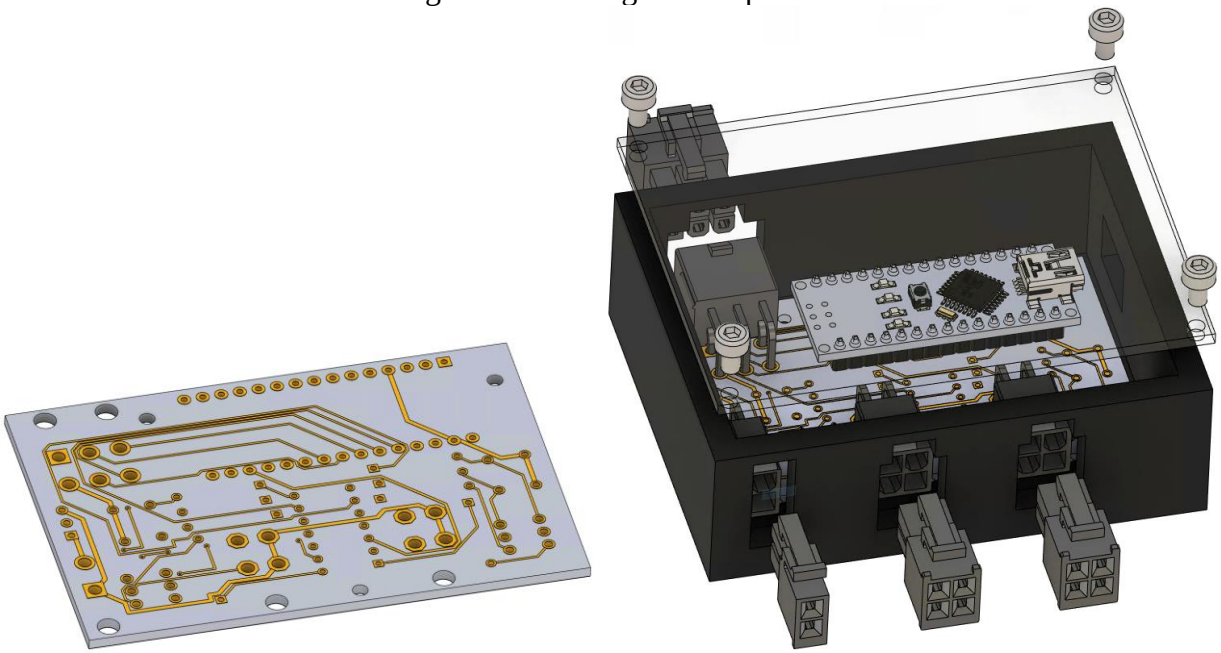

Figure 5.7 Electronics Assembly

5.2.1.3 Damper Control Circuit Justification

The damper valves are adjusted by varying their input current to control how hard/soft their compression is. The valves are fully closed at 0mA, which results in the dampers being at full compression by default. When current is applied, the valves are proportionally opened, which lowers their compression. According to the damper's dynamometer test data, the valves are fully open around 700mA. Therefore, the desired function of the damper control circuit is shown below.

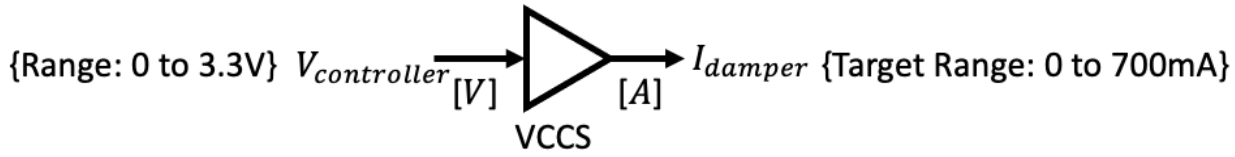

Figure 5.8 Damper Control Circuit Black Box Diagram

The SPICE circuit below models a single damper control circuit. The input ($V_{control}$) has a range from 0 to 3.3V and is set by an analog output pin on the microcontroller. The output (I_{damper}) has a range from 0 to 702mA and is directly proportional to $V_{control}$. The target max current value is 700mA.

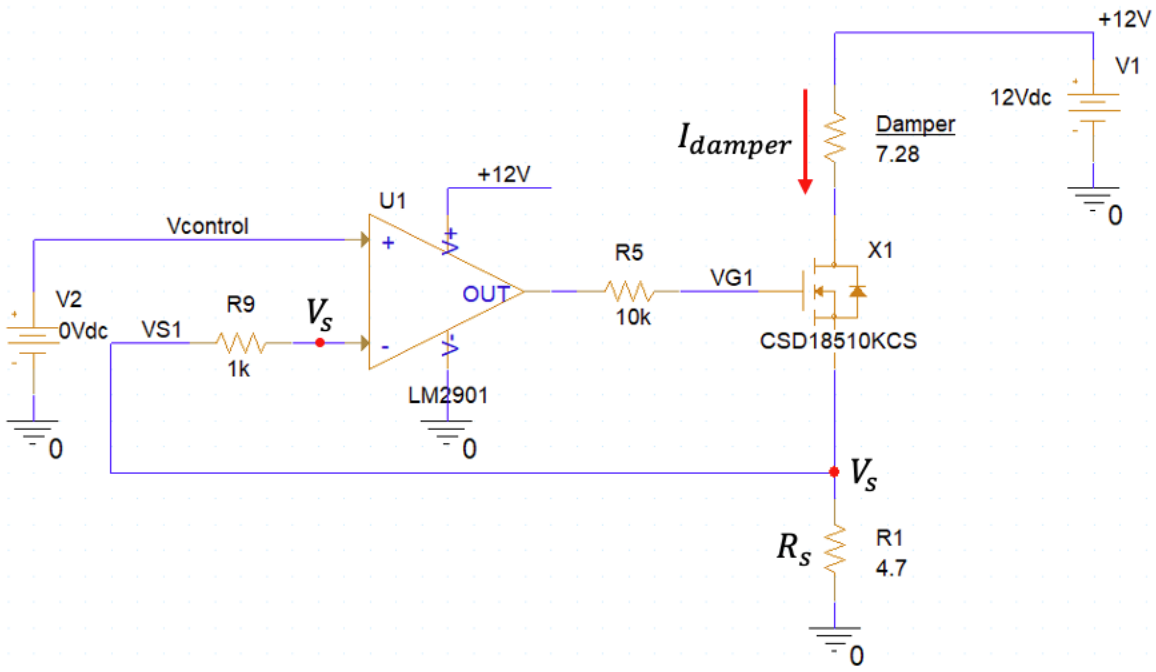

Figure 5.9 Damper Control Circuit Schematic

Based on the damper control circuit schematic, the current provided to each damper can be derived as follows:

$$V_s \approx V_{control}$$

$$I_{damper} = \frac{V_s - 0}{R_s}$$

$$I_{damper} = \frac{V_{control}}{R_s}$$

Using the equation above, the maximum damper current can be calculated based on the maximum controller output of 3.3V:

$$\frac{3.3V}{4.7\Omega} = 702mA$$

Therefore, the maximum current provided to a single damper is 702mA, which is very close to the target maximum damper current of 700mA. Notably, the absolute maximum current rating for each damper is 885mA, so this maximum current supply rating is safe.
The figure below was generated from a PSpice simulation of the damper control circuit. The control voltage was swept from 0 to 3.3V in 0.1V increments. As seen in the simulation output graph, the damper current proportionally scales from 0 to 702mA.

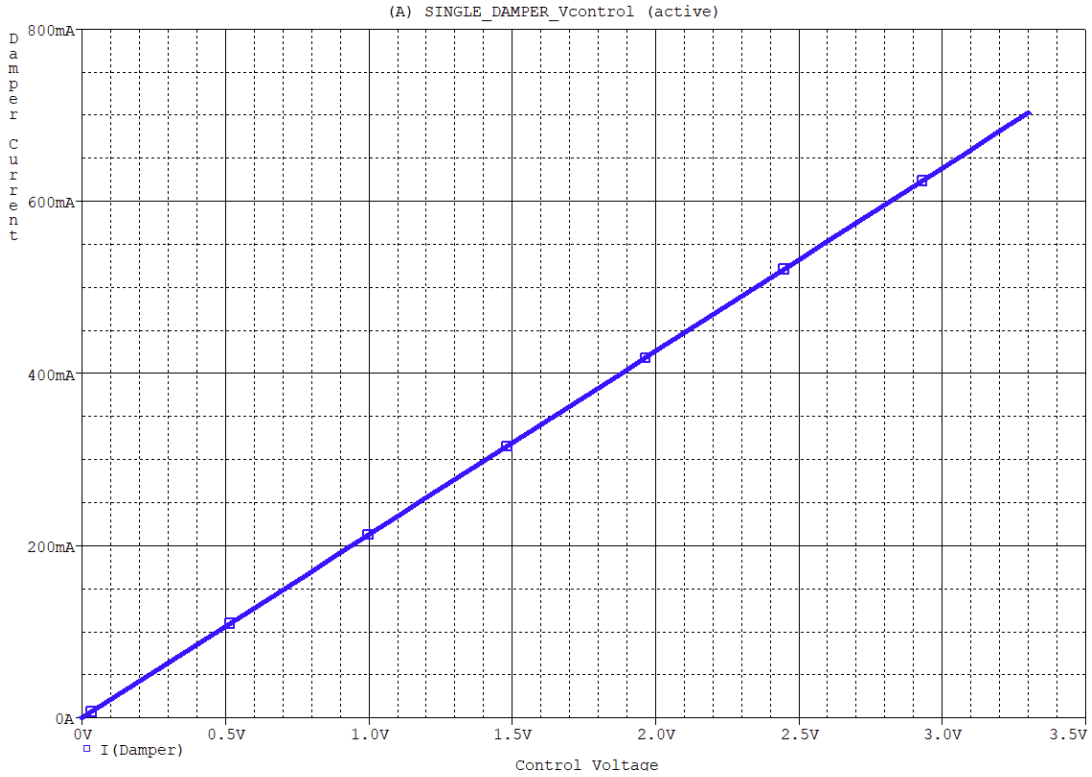

Figure 5.10 Damper Current vs. Control Voltage (PSpice)

Conclusively, the damper control circuit will linearly relate the input control voltage of 0 to 3.3V to the output damper current of 0 to 702mA.

5.2.1.4 Battery Justification

The system was modeled in PSpice, and the operating point was calculated for the circuit under max load. Max load parameters are summarized in the table below.

Table 5.2.1 Max Load Parameters

Parameter	Max Load	Unit
Microcontroller Current Draw	140	mA
Damper Current Draw	702.5	mA
Microcontroller GPIO Output	3.3	V
Potentiometer Resistance	1	kΩ

According to its datasheet, the maximum current draw for the STM32L412KVU6 microcontroller is 140mA. The actual current draw is expected to be much less, as the microcontroller is used to source very small currents to high impedance outputs. The damper current draw has been derived from the damper control circuit discussed in section 5.2.1.3. The microcontroller GPIO output, which is used as the damper control circuit input, can be set to a maximum of 3.3V according to the microcontroller datasheet. Finally, the potentiometers will draw the most power at their lowest resistance, which is 1kΩ according to the datasheet.

Based on the parameters mentioned above, the table below summarizes the PSpice simulation results of the power consumption for the system's most notable components.

Table 5.2.2 Max Power Draw Breakdown

Component	Quantity	Max Power Draw (W)
Microcontroller	1	0.464
Damper	4	14.372
N-MOSFET	4	10.072
N-MOSFET Source Resistor	4	9.280
Other	-	1.522
Total	**-**	**35.71**

Based on the breakdown of the max power draw, if the system were to run at max load for 4 hours (the length of the Baja endurance event), a battery of at least a 11.9 Amp-hour capacity would be required. Therefore, the system will be powered by a standard 12 Amp-hour lead acid battery.

$$I_{max} = \frac{P_{max}}{V_{max}} = \frac{35.71\ W}{12\ V} = 2.976\ A$$

$$2.796\ A\ \times\ 4\ hr = 11.9\ Ah$$

Battery Capacity ≥ 11.9 Amp-hours

5.2.2 Software Functionality

5.2.2.1 Microcontroller Justification

The STM32L412KB Nucleo-32 microcontroller was chosen because of its low power consumption, hardware debugging capabilities, and IDE capabilities. As seen in the weighted decision matrix below, the Nucleo is a clear choice over its competition: the Arduino and TEENSY microcontrollers.

Table 5.2.3 Microcontroller Weighted Decision Matrix

		Arduino		Teensy		Nucleo	
Criteria	**Weighting**	**Score**	**Total**	**Score**	**Total**	**Score**	**Total**
Packaging	3	5	15	3	9	4	12
Debugging	5	0	0	0	0	5	25
IDE	3	0	0	0	0	5	15
Power Consumption	4	3	12	2	8	5	20
Cost	1	5	5	1	1	3	3
Total	**16**		**32**		**18**		**75**

5.2.2.2 Algorithm Justification

To analyze and develop the algorithm that will control the amount of current sent to the damper, a MATLAB model is being used to simulate performance and any physical constraints that gets tested in the future. The MATLAB model is a model of one corner of the Baja car, namely the wheel and quarter-car body capable of moving independently in the y-direction.

It was decided that the algorithm would reference dyno data from 2019 on the current dampers with 5/8” shafts to get an idea of how damping should look. It was decided that the data from the dampers with 7/8” shafts and Live Valves, which were made for much heavier vehicles, would be used to guide modifications to adjust the dampers to behave more appropriately for the Baja SAE vehicle. In the MATLAB model, damping was referenced by finding the damping coefficient as a function of damper velocity. These functions were extrapolated to fill in the damping range not covered by the “mid,” “closed,” and “open” settings.

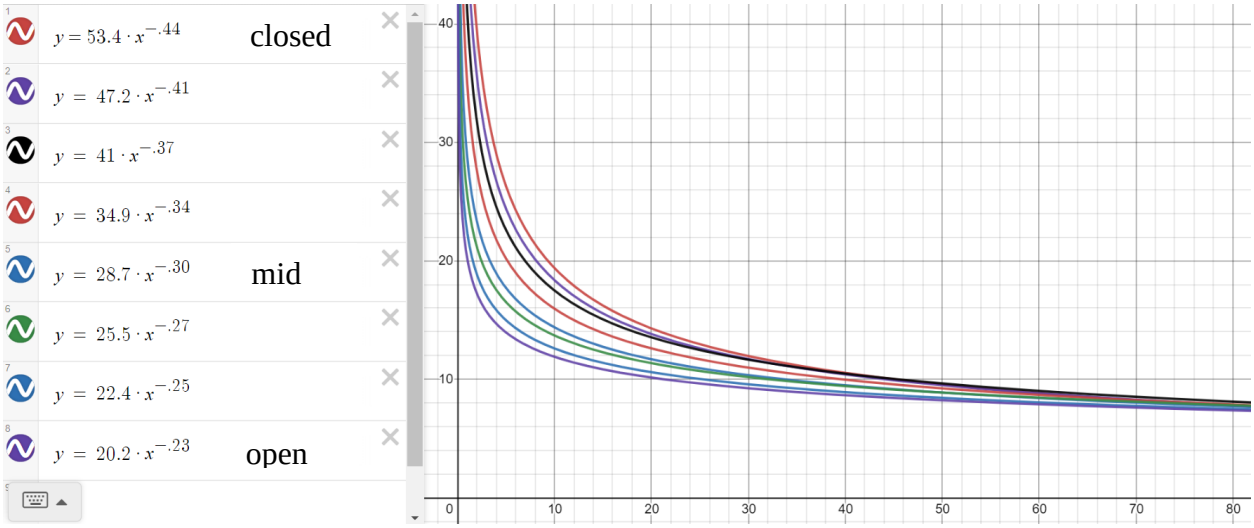

Figure 5.11 Extrapolated Damper Coefficient, c [lbs*s/in] vs Damper Velocity, v [in/s]

The coefficient and exponent in the exponential curve-fits to the left in Figure 5.11 were then put in a matrix in MATLAB as shown in Figure 5.12

```
%-------------- Extrapolated data of 5/8 shocks ----------------%
% The power formula: cs = A_cs * s_vel ^ B_cs
%
%               Iv      A_cs    B_cs    low_speed
cs_lookup = [   0       53.4    -.44    99;
                0.1     47.2    -.41    92;
                0.2     41      -.37    85;
                0.3     34.9    -.34    78;
                0.4     28.7    -.30    71;
                0.5     25.5    -.27    64;
                0.6     22.4    -.25    57;
                0.7     20.2    -.23    50];
```

Figure 5.12 Damping Coefficient Lookup Table and Extrapolated Formula

The first column is not used in the code and just for reference to read which row is for which current setting. The right-most column stores the damping coefficient that was estimated to be at low speeds which is defined as shock velocity less than 1 in/s.

A couple of algorithms we have tested are shown in Figure 5.13.

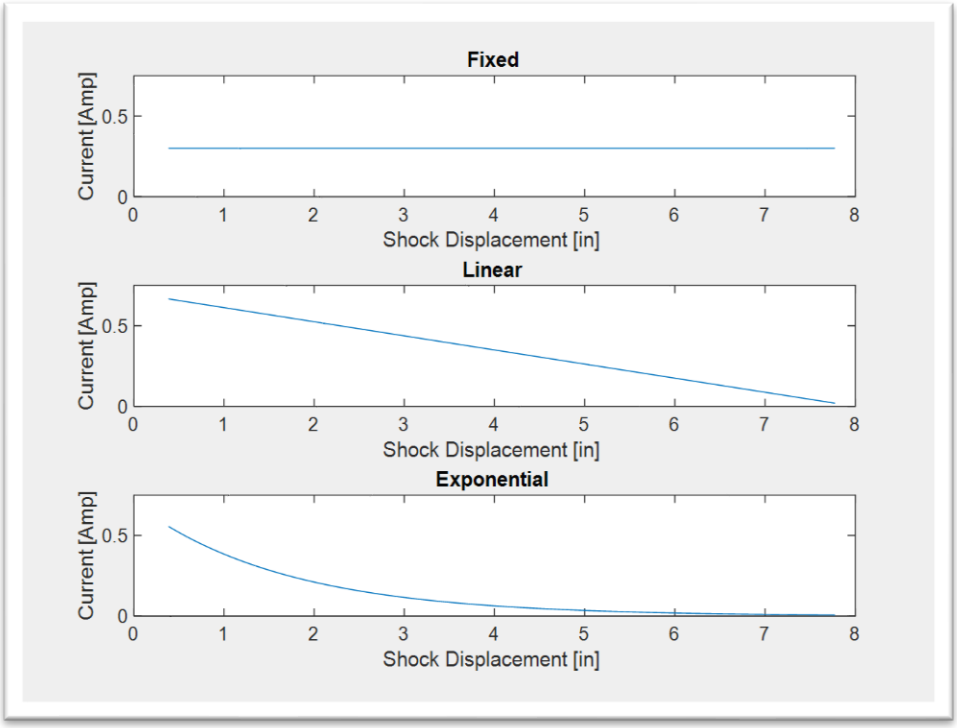

Figure 5.13 Three different current control tests

First, there is the passive damper where one valve setting is picked and that's all that can be used in the duration of the simulation. Next, there is the Linear algorithm where the relationship between current and shock displacement is inversely proportionate. At bottom-out where Shock Displacement is 8in, the current to output is zero so that the damper is at its hardest setting. At top-out where Shock Displacement is 0in, the current to give the Live Valve is 0.7A so that the damper is at its softest setting. Lastly, the Exponential algorithm is a variation of this strategy but with a more aggressive ramp up to the hardest damper setting as the damper compresses towards bottom out.

Currently, the performance of the MATLAB simulation is lacking. The hope is that this is not a reflection of how the concept is working due to a bug in the MATLAB code. On the other hand, it could mean there is a lot more work to be done to optimize the algorithm.

Another culprit is whether the road profiles that were made in MATLAB is similar enough to what would actually be experienced by the Baja car. A couple road profiles that were tested are shown in Figure 5.14.

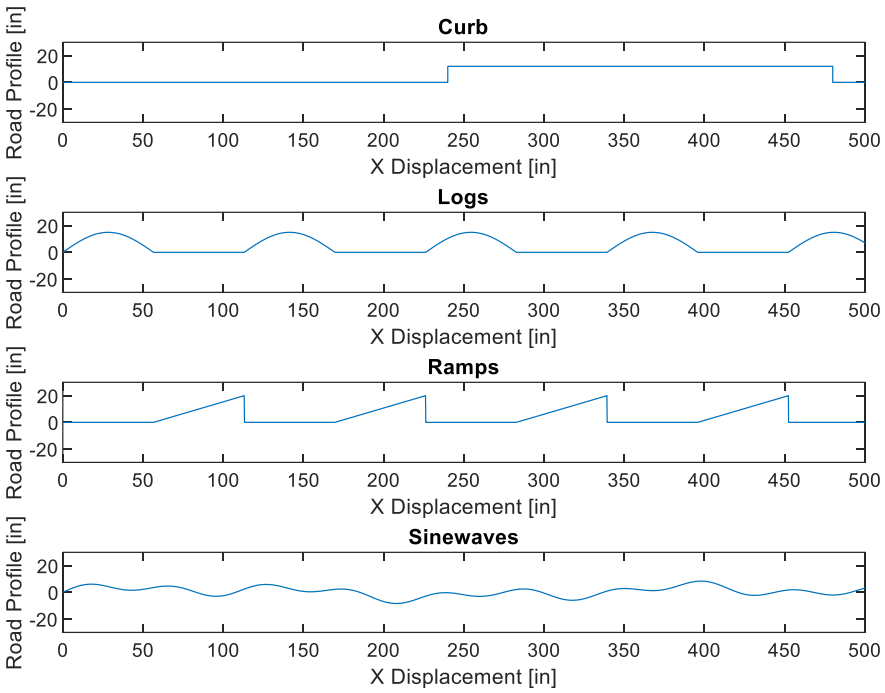

Figure 5.14 Road Profiles in MATLAB

To evaluate performance of the algorithm, we used two distribution graphs and three data points that characterize ride comfort and ground contact:

1. Unsprung mass upward acceleration histogram [in/s^2]
2. Damper displacement histogram [in]
3. Bottom-out events
4. Total upward acceleration experienced [in/s^2]
5. Unsprung mass average height [in]

All road profiles were tested but results were marginally different between the Exponential SAS algorithm and the results from the Passive simulation. The road profile that shows the most optimistic result is the “Ramp” road profile in Figure 5.14. An animation is shown below of that simulation.

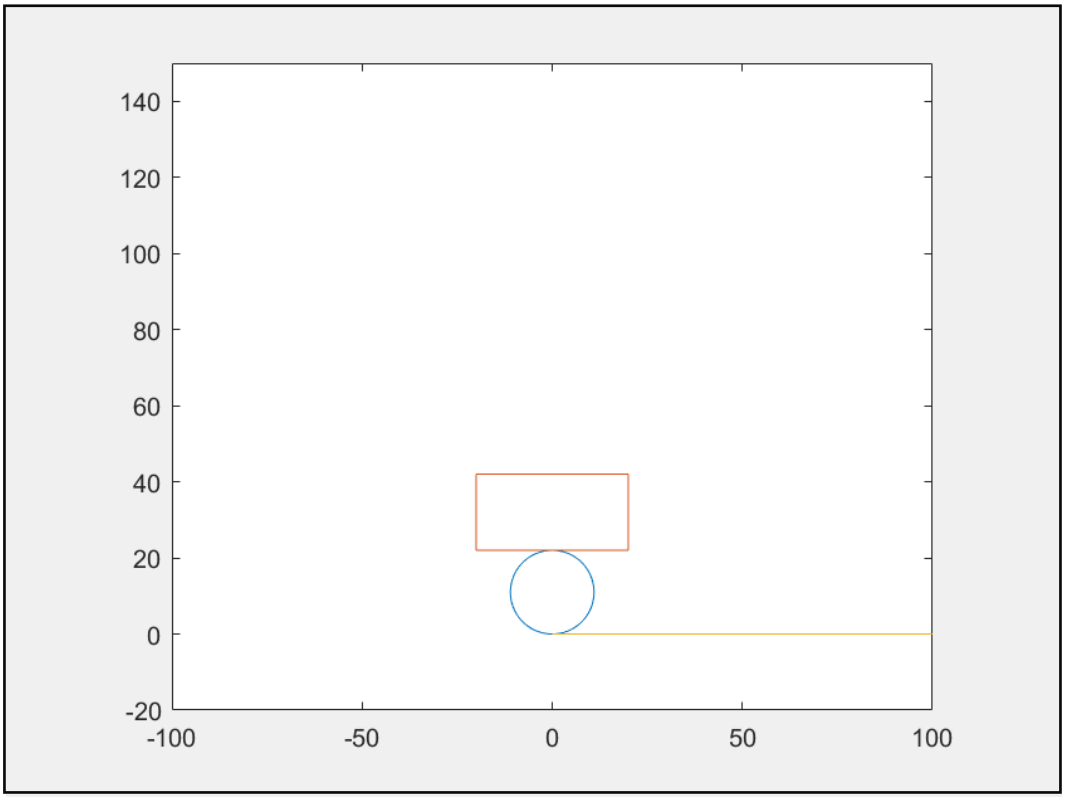

Figure 5.15 Simulation of Exponential SAS on "Ramp"-like road profile

The results from this simulation are shown below.

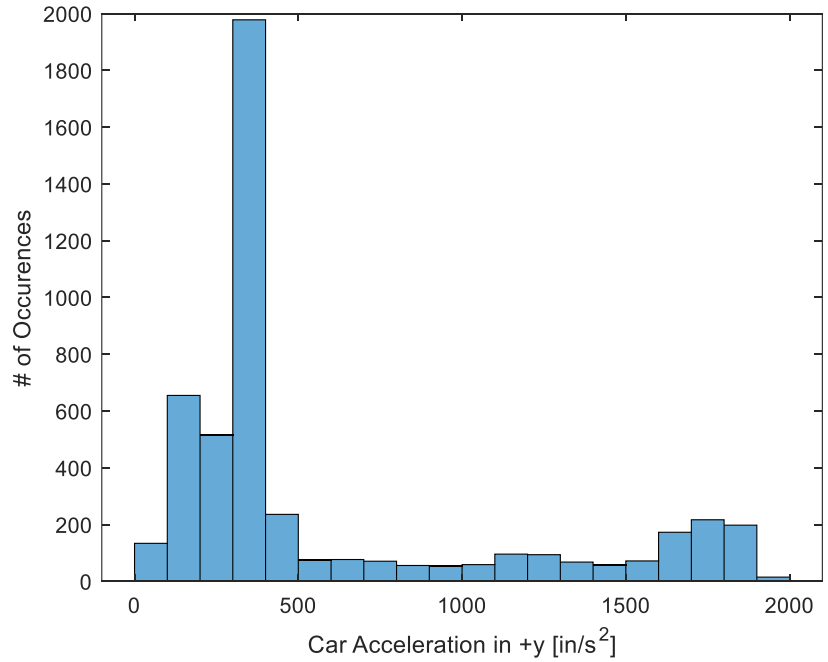

Figure 5.16 Exponential SAS: Distribution of unsprung mass upward acceleration

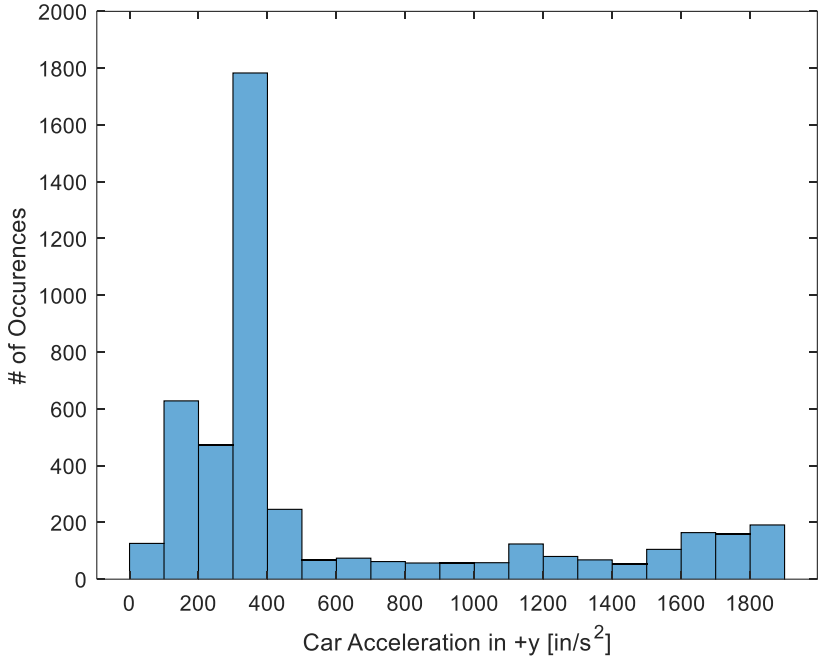

Figure 5.17 Passive suspension: Distribution of unsprung mass upward acceleration

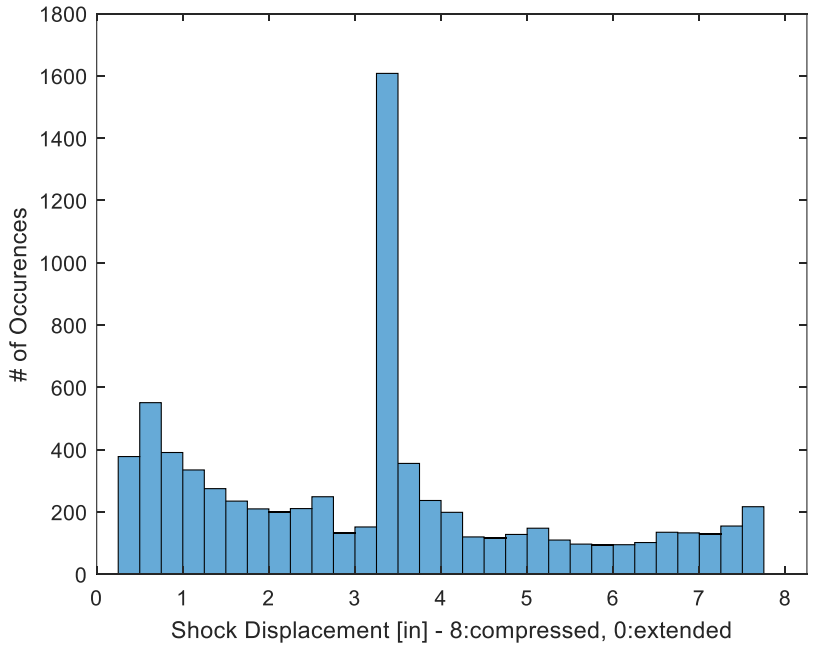

Figure 5.18 Exponential SAS: Distribution of damper displacement

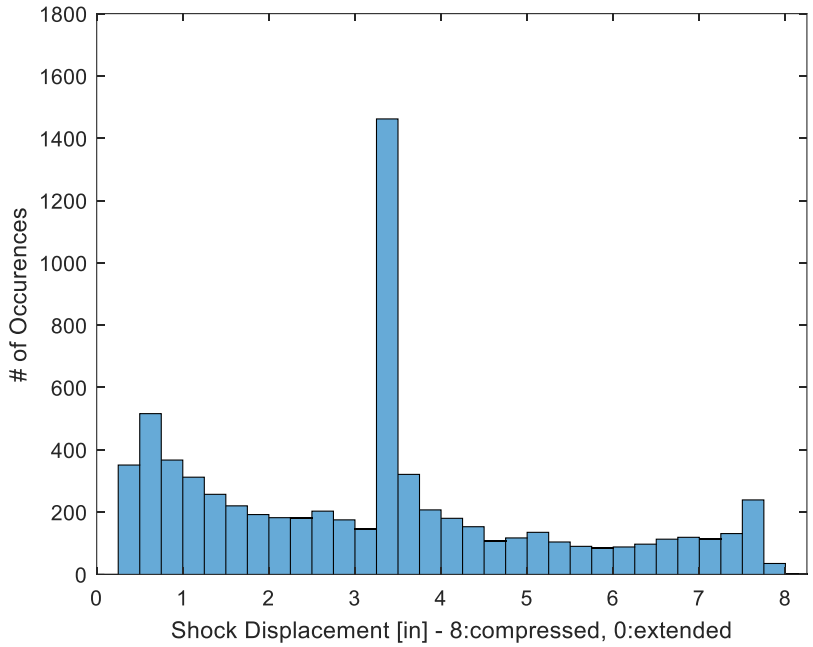

Figure 5.19 Passive suspension: Distribution of damper displacement

Table 5.2.4 Algorithm performance characteristics

	Exponential SAS	**Linear SAS**	**PASSIVE**
Bottom Out Events	0	0	0
Total Upward Accel. Experienced [in/s^2]	**2.94*10^6**	**3.04*10^6**	**2.74*10^6**
Average Sprung Mass Height [in]	**1.66**	**0.997**	**2.17**

Comparing first the two unsprung mass acceleration histograms, the goal is to essentially reduce high end accelerations because the high accelerations are what cause discomfort. Currently, they both look troublingly similar and the SAS simulation actually shows worse results. Accelerations up to 2000 in/s^2 are shown. This is reflected in Table 5.2.4, where the overall total of upward acceleration is higher with the SAS algorithms compared to the passive, single-setting strategy.

Moving onto the damper displacement histograms, the goal is to eliminate bottom out events and reduce the number of times the damper reaches 8 in of travel. This was successfully accomplished, in fact. As discussed before, bottom out events are the main cause of driver discomfort. Figure 5.19, displacements do reach up past 7.75 in.

Examining Table 5.2.4, bottom out is not reached on the simulated road profile and thus the number of bottom out events does not represent much information. This parameter can show very easily on other road profiles if the SAS algorithm is successful at reducing bottom-out

events. It was a hope to reduce overall accelerations, but these numbers are starting to suggest a byproduct of eliminating high-end, bottom-out accelerations will result in more overall upward acceleration. This is to be further investigated. The hope to compare average sprung mass height over a simulation period is that it would help represent amount of ground contact. If the car was lower to the ground overall, that means less airtime, making more contact with the ground.

In summary, there is much work left to do to show effectiveness and determine whether or not the SAS system currently being presented can reach the design goals. That has not been shown yet, but with more tuning time and development, the hope is that the current MATLAB model has some bugs and is not an accurate reflection of the SAS system. One reason this could be true is that the model should be spending more time in softer settings but lower accelerations are not much more frequent. The rebound settings in the model are also not tuned yet, so that might very well change these results.

5.3 Summary Cost Analysis

Since the damper and valve actuator were provided by Fox Factory, the primary components that needed to be purchased included the springs, electronics hardware, and data collection equipment. A detailed parts list is provided in Appendix E, the Indented Bill of Materials (iBOM). The springs were chosen but not purchased due to the test-bench setup of this project.

Table 5.3.1 Mechanical Summary Cost Analysis

Mechanical			
Assembly	**Subassembly**	**Cost**	**Procure/Manufacture**
Coilover Damper	---	---	---
	Damper	---	Procured from Fox Factory
	Valve Actuator	---	Procured from Fox Factory
	2.5” ID x 14” Length Springs 70 lbf/in	$60/ea.	F-O-A Off-Road Shocks
Total	**---**	**$120**	**---**

Table 5.3.2 Electronics Summary Cost Analysis

Electrical			
Assembly	**Subassembly**	**Cost**	**Procure/Manufacture**
PCB	---	---	---
	Components	$39.99	Order from Digikey
	Circuit Board	$7.65	Order from JLCPCB
	Integration	$0.00	3D print at home
Potentiometers	---	$0.00	Order from TE Connectivity
Wiring Harness	---	$0.00	Solder in machine shop
Total	**---**	**$47.64**	**---**

5.4 Concerns

Since the damper that was procured is not directly compatible with the Baja car's suspension, it will not be a direct fit. It will require modifications including shortening the damper body, installing a softer shim stack, and new springs with a lower spring rate. The damper modifications are discussed in Chapter 6, but concerns include the accuracy of the modifications and the quality of the damper rebuild. Additionally, long coilover springs with low spring rates are difficult to source for the 2.5 inch body, and lack of appropriate spring rates for the lighter mini-UTV application would lead to poor handling characteristics.

The microcontroller's digital-to-analog converter (DAC) may not output a perfect 3.3V maximum signal. If the maximum voltage is below 3.3V, the damper control circuit will not output the full range of currents derived in section 5.2.1.3. If the maximum output current is less that desired, the damper control circuit may need adjustment to compensate for a lower range of control voltages.

5.5 Design Changes After CDR

5.5.1 Mechanical

5.5.1.1 Damper Shims and Shaft

The dampers that were adapted with a Live Valve come stock on a Yamaha YXZ; a full-size, 2-seater side-by-side. After some initial testing, it became clear that they are tuned to be way too stiff for a lightweight Baja racecar and had to be re-shimmed to provide much less damping force. To do this, the damper was taken apart and the valve code of the main piston was documented and re-valved. However, if the main piston code is made too soft there will not be enough pressure behind it to prevent cavitation, and even after softening the main piston as much as possible, the damper was still not soft enough. The 7/8" shaft was then replaced with a 5/8" shaft so that for the same amount of stroke, less oil flows through the base valve, further softening the damper without the risk of cavitation. This provided the desired range of damping that is suitable for the Baja car.

Figure 5.20 New Shim Stack

5.5.2 Software

5.5.2.1 State Space Models

The proportional control algorithm presented at CDR adjusted the damping coefficient linearly depending on the position of each damper. The algorithm was limited in this way as a proof of concept to tune the MATLAB model that was being used. However, this algorithm does not account for other states of the overall system to consider vehicle pitch and height in addition to their respective velocities and accelerations. Therefore, to gain a better understanding of the system, state space models have been produced for both the quarter-car and half-car models. Section 5.6 covers the state space models more in-depth.

5.6 State Space Models

The purpose of creating a state space model for the system is to analyze the controllability and observability of the system, and to create an accurate description of the system's response to any input terrain. This information can be useful in determining which sensors would work with the SAS system, and it will allow future engineers to observe every aspect (or state) or the system in MATLAB to help tune the system. Additionally, a MATLAB model can be used to determine the vertical and rotational accelerations experienced by the driver, which can tell how comfortable they are. State space models will only be developed for the half car and quarter car because of the system complexity. However, these models can be expanded to the full car using the same concepts.

5.6.1 Descriptions

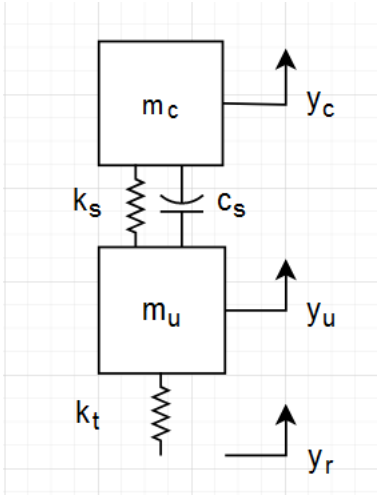

Figure 5.6.1.1 Simplified Quarter-Car Model

A state equation and a transfer function for the quarter-car model can be derived from the system shown in figure 5.6.1.1, and the symbols are described in the table below.

Table 5.6.1.1 Quarter-Car Model Symbol Descriptions

Symbol	Definition
y_c	Vertical chassis position
y_u	Vertical un-sprung mass (wheel) position
y_r	Vertical ground position
k_s	Suspension spring constant
k_t	Tire spring constant
c_s	Damping coefficient
m_c	Chassis mass
m_u	Un-sprung (wheel) mass

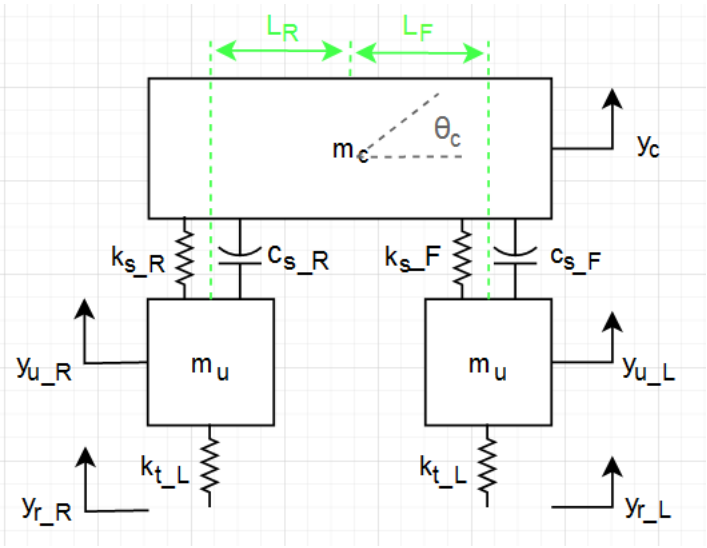

Figure 5.6.1.2 Half-Car Model

The quarter-car model in figure 5.6.1.1 can be expanded to a half-car model with the addition of another quarter-car. The half-car model is shown in figure 5.6.1.2 above. As seen in the figure, the individual front and rear quarter-car models remain the same, but the model includes new constants and variables. The quarter-car symbols are labelled with additional subscripts to designate "front" and "rear" components. The additional half-car symbols are described in the table below.

Table 5.6.1.2 Half-Car Model Symbol Descriptions

Symbol	Definition
L_F	Distance between front damper and center of mass
L_R	Distance between rear damper and center of mass
θ_c	Chassis pitch

5.6.2 Formulas

Quarter-Car

This section describes the formulas used to derive the quarter-car and half-car state equations.

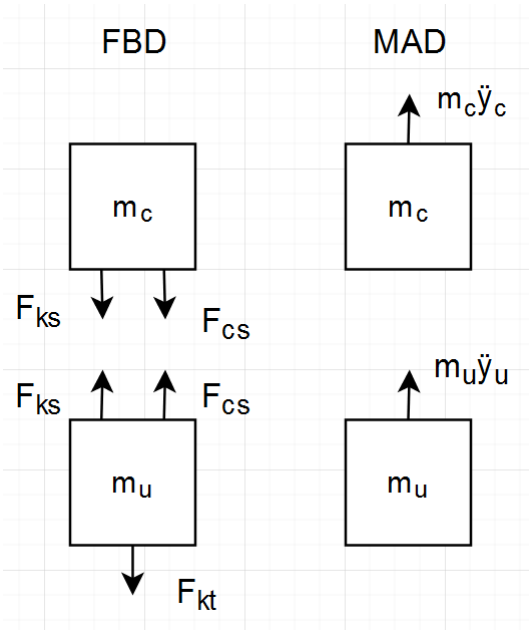

Figure 5.6.2.1 Quarter-Car Free Body Diagram and Mass Acceleration Diagram

The quarter-car free body diagram and mass acceleration diagram in figure 5.6.2.1 were used to derive the following formulas for vertical chassis acceleration and vertical wheel acceleration. The "y" symbols have been replaced with the "z" symbol, so they won't get confused with the output "y" symbols in the state equation.

Vertical Chassis Acceleration

$$\ddot{z}_c = \frac{-c_s}{m_c}\dot{z}_c - \frac{k_s}{m_c}z_c + \frac{c_s}{m_c}\dot{z}_u + \frac{k_s}{m_c}z_u$$

Vertical Wheel Acceleration

$$\ddot{z}_u = \frac{-c_s}{m_u}\dot{z}_u - \frac{(k_s + k_t)}{m_u}z_u + \frac{c_s}{m_u}\dot{z}_c + \frac{k_s}{m_u}z_c + \frac{k_t}{m_u}z_r$$

Half-Car

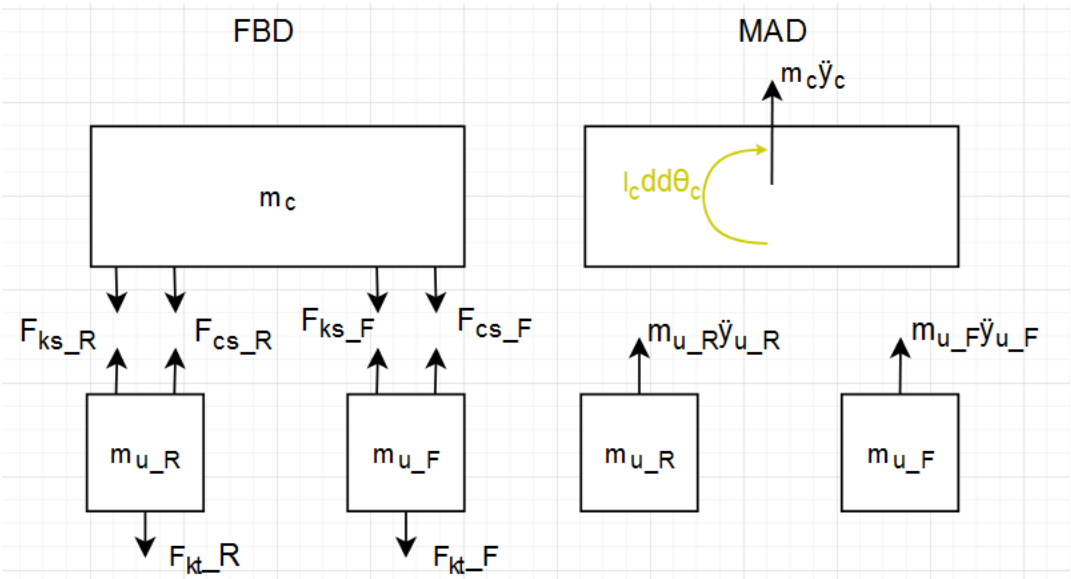

Figure 5.6.2.2 Half-Car Free Body Diagram (Left) and Mass Acceleration Diagram (Right)

The half-car free body diagram and mass acceleration diagram in figure 5.6.2.2 were used to derive the following formulas for vertical chassis acceleration, vertical front and rear wheel accelerations, and angular chassis acceleration (pitch). The "y" symbols have been replaced with the "z" symbol, so they won't get confused with the output "y" symbols in the state equation.

Vertical Chassis Acceleration

$$\ddot{y}_c = \frac{1}{m_c}[c_{sR}\dot{y}_{uR} + k_{sR}y_{uR} - c_{sR}\dot{y}_c - k_{sR}y_c + c_{sR}L_R\sin(\dot{\theta}_c) + k_{sR}L_R\sin(\theta_c) + c_{sF}\dot{y}_{uF} + k_{sF}y_{uF} - c_{sF}\dot{y}_c - k_{sF}y_c - c_{sF}L_F\sin(\dot{\theta}_c) - k_{sF}L_F\sin(\theta_c)]$$

Using sine approximation:

$$\ddot{z}_c = \frac{-(k_{sF}+k_{sR})}{m_c}z_c + \frac{-(c_{sF}+c_{sR})}{m_c}\dot{z}_c + \frac{k_{sF}}{m_c}z_{uF} + \frac{c_{sF}}{m_c}\dot{z}_{uF} + \frac{k_{sR}}{m_c}z_{uR} + \frac{c_{sR}}{m_c}\dot{z}_{uR} + \frac{(-k_{sF}L_F + k_{sR}L_R)}{m_c}\theta_c + \frac{(-c_{sF}L_F + c_{sR}L_R)}{m_c}\dot{\theta}_c$$

Vertical Front Wheel Acceleration

$$\ddot{y}_{uF} = \frac{1}{m_{uF}}[-c_{sF}\dot{y}_{uF} - (k_{sF}+k_{tF})y_{uF} + c_{sF}\dot{y}_c + k_{sF}y_c + c_{sF}L_F\sin(\dot{\theta}_c) + k_{sF}L_F\sin(\theta_c) + k_{tF}y_{rF}]$$

Using sine approximation:

$$\ddot{z}_{uF} = \frac{k_{sF}}{m_{uF}} z_c + \frac{c_{sF}}{m_{uF}} \dot{z}_c + \frac{-(k_{sF} + k_{tF})}{m_{uF}} z_{uF} + \frac{-c_{sF}}{m_{uF}} \dot{z}_{uF} + \frac{k_{sF} L_F}{m_{uF}} \theta_c + \frac{c_{sF} L_F}{m_{uF}} \dot{\theta}_c + \frac{k_{tF}}{m_{uF}} z_{rF}$$

Vertical Rear Wheel Acceleration

$$\ddot{y}_{uR} = \frac{1}{m_{uR}} [-c_{sR}\dot{y}_{uR} - (k_{sR} + k_{tR}) y_{uR} + c_{sR}\dot{y}_c + k_{sR} y_c - c_{sR} L_R \sin(\dot{\theta}_c) - k_{sR} L_R \sin(\theta_c) + k_{tR} y_{rR}]$$

Using sine approximation:

$$\ddot{z}_{uR} = \frac{k_{sF}}{m_{uR}} z_c + \frac{c_{sF}}{m_{uR}} \dot{z}_c + \frac{-(k_{sR} + k_{tR})}{m_{uR}} z_{uR} + \frac{-c_{sR}}{m_{uR}} \dot{z}_{uR} + \frac{-k_{sR} L_R}{m_{uR}} \theta_c + \frac{-c_{sR} L_R}{m_{uR}} \dot{\theta}_c + \frac{k_{tR}}{m_{uR}} z_{rR}$$

Angular Chassis Acceleration (Pitch)

$$\ddot{\theta}_c = \frac{1}{I_G} [-c_{sR} L_R \dot{y}_{uR} - k_{sR} L_R y_{uR} + c_{sR} L_R \dot{y}_c + k_{sR} L_R y_c - c_{sR} {L_R}^2 \sin(\dot{\theta}_c) - k_{sR} {L_R}^2 \sin(\theta_c) + c_{sF} L_F \dot{y}_{uF} + k_{sF} L_F y_{uF} - c_{sF} L_F \dot{y}_c - k_{sF} L_F y_c - c_{sF} {L_F}^2 \sin(\dot{\theta}_c) - k_{sF} {L_F}^2 \sin(\theta_c)]$$

Using sine approximation:

$$\ddot{\theta}_c = \frac{(-k_{sF} L_F + k_{sR} L_R)}{I_G} z_c + \frac{(-c_{sF} L_F + c_{sR} L_R)}{I_G} \dot{z}_c + \frac{k_{sF} L_F}{I_G} z_{uR} + \frac{c_{sF} L_F}{I_G} \dot{z}_{uF} + \frac{-k_{sR} L_R}{I_G} z_{uR} + \frac{-c_{sR} L_R}{I_G} \dot{z}_{uR} + \frac{-(k_{sF} L_F^2 + k_{sR} L_R^2)}{I_G} \theta_c + \frac{-(c_{sF} L_F^2 + c_{sR} L_R^2)}{I_G} \dot{\theta}_c$$

5.6.3 State Variables

Quarter-Car

State Vectors

The state vectors of the system were chosen to be the vertical height of the chassis and the vertical height of the wheel. The chassis height also represents the height of the driver. The state vectors are described below.

Car Height

$x_1 = z_c = y_1$ $\quad\quad$ $\dot{x}_1 = x_2$

$x_2 = \dot{z}_c$ $\quad\quad$ $\dot{x}_2 = \ddot{z}_c$

Wheel Height

$x_3 = z_u = y_2$ $\quad\quad$ $\dot{x}_3 = x_4$

$x_4 = \dot{z}_u$ $\dot{x}_4 = \ddot{z}_u$

Input Vectors

The only quarter-car system input is the vertical height of the ground. Therefore, functions can be generated to represent various environments and terrains. For instance, a noise function can represent rocky terrain, and a sine function can represent hilly terrain. This also means that a step input function can give insight into the stability and driver comfort of the system. The input vector is described below.

Ground Height

$u = z_r$

Output Vectors

The output vector was chosen to be the vertical height of the chassis and the vertical height of the wheel. The chassis height is also the driver height, which means the vertical chassis acceleration can provide an excellent measurement of the comfort of the driver. One of the main goals of the SAS system is to enhance driver comfort by reducing vertical acceleration, so this is a very important aspect of the system to analyze. Furthermore, the vertical height of the wheel gives insight into how the suspension responds to different inputs. To explain, the wheel height should change very quickly when the car is going over rocky terrain to reduce the vertical accelerations of the driver, and the wheel height should change slowly when the car is going over flat ground to keep the chassis steady. The output vector is described below.

Vertical Car Height

$y_1 = z_c$

Vertical Wheel Height

$y_2 = z_u$

Half-Car

State Vectors

The state vectors of the system were chosen to be the vertical height of the chassis, the vertical height of both wheels, and the angular chassis acceleration (pitch). These state vectors are like the quarter-car model, but they also include pitch with the addition of a new dimension to the model. The state vectors are described below.

Car Height

$x_1 = z_c = y_1$ $\dot{x}_1 = x_2$

$x_2 = \dot{z}_c$ $\dot{x}_2 = \ddot{z}_c$

Front Wheel Height

$x_3 = z_{uF} = y_2$ $\dot{x}_3 = x_4$

$x_4 = \dot{z}_{uF}$ $\dot{x}_4 = \ddot{z}_{uF}$

Rear Wheel Height

$x_5 = z_{uR} = y_3$ $\quad\quad$ $\dot{x}_5 = x_6$

$x_6 = \dot{z}_{uR}$ $\quad\quad$ $\dot{x}_6 = \ddot{z}_{uR}$

Pitch

$x_7 = \theta_c = y_4$ $\quad\quad$ $\dot{x}_7 = x_8$

$x_8 = \dot{\theta}_c$ $\quad\quad$ $\dot{x}_8 = \ddot{\theta}_c$

Input Vectors

The half-car system inputs are the vertical heights of the ground under both the front and rear wheels. Like the quarter-car model, functions can be generated to represent various environments and terrains. The input vector is described below.

Ground Heights

$u_1 = z_{rF}$

$u_2 = z_{rR}$

Output Vectors

Like the quarter-car model, the output vector was chosen to be the vertical height of the chassis and the vertical height of the wheels. However, the half-car model will output front and rear wheel heights, and another output was chosen to be the pitch of the chassis. The pitch of the chassis is also the pitch of the driver, and this is important to analyze because it gives the angular acceleration of the driver. This is significant because a main goal of the SAS system is to reduce the angular acceleration of the driver to enhance driver comfort. The output vector is described below.

Vertical Car Height

$y_1 = z_c$

Vertical Wheel Heights

$y_2 = z_{uF}$

$y_3 = z_{uR}$

Angular Car Pitch

$y_4 = \theta_c$

5.6.4 State Equations

Quarter-Car
Equations

$$\begin{bmatrix}\dot{x}_1\\ \dot{x}_2\\ \dot{x}_3\\ \dot{x}_4\end{bmatrix} = \begin{bmatrix} 0 & 1 & 0 & 0 \\ -\frac{k_s}{m_c} & -\frac{c_s}{m_c} & \frac{k_s}{m_c} & \frac{c_s}{m_c} \\ 0 & 0 & 0 & 1 \\ \frac{k_s}{m_u} & \frac{c_s}{m_u} & -\frac{(k_s+k_t)}{m_u} & -\frac{c_s}{m_u}\end{bmatrix}\begin{bmatrix}x_1\\ x_2\\ x_3\\ x_4\end{bmatrix} + \begin{bmatrix}0\\ 0\\ 0\\ \frac{k_t}{m_u}\end{bmatrix}u$$

$$\begin{bmatrix}y_1\\ y_2\end{bmatrix} = \begin{bmatrix}1 & 0 & 0 & 0\\ 0 & 0 & 1 & 0\end{bmatrix}\begin{bmatrix}x_1\\ x_2\end{bmatrix} + \begin{bmatrix}0\\ 0\end{bmatrix}u$$

Matrices

$$A = \begin{bmatrix} 0 & 1 & 0 & 0 \\ -\frac{k_s}{m_c} & -\frac{c_s}{m_c} & \frac{k_s}{m_c} & \frac{c_s}{m_c} \\ 0 & 0 & 0 & 1 \\ \frac{k_s}{m_u} & \frac{c_s}{m_u} & -\frac{(k_s+k_t)}{m_u} & -\frac{c_s}{m_u}\end{bmatrix}$$

$$B = \begin{bmatrix}0\\ 0\\ 0\\ \frac{k_t}{m_u}\end{bmatrix}$$

$$C = \begin{bmatrix}1 & 0 & 0 & 0\\ 0 & 0 & 1 & 0\end{bmatrix}$$

$$D = \begin{bmatrix}0\\ 0\end{bmatrix}$$

Half-Car

Equations

$$\begin{bmatrix}\dot{x}_1\\ \dot{x}_2\\ \dot{x}_3\\ \dot{x}_4\\ \dot{x}_5\\ \dot{x}_6\\ \dot{x}_7\\ \dot{x}_8\end{bmatrix} = \begin{bmatrix} 0 & 1 & 0 & 0 & 0 & 0 & 0 & 0 \\ \frac{-(k_{sF}+k_{sR})}{m_c} & \frac{-(c_{sF}+c_{sR})}{m_c} & \frac{k_{sF}}{m_c} & \frac{c_{sF}}{m_c} & \frac{k_{sR}}{m_c} & \frac{c_{sR}}{m_c} & \frac{-k_{sF}L_F+k_{sR}L_R}{m_c} & \frac{-c_{sF}L_F+c_{sR}L_R}{m_c} \\ 0 & 0 & 0 & 1 & 0 & 0 & 0 & 0 \\ \frac{k_{sF}}{m_{uF}} & \frac{c_{sF}}{m_{uF}} & \frac{-(k_{sF}+k_{tF})}{m_{uF}} & \frac{-c_{sF}}{m_{uF}} & 0 & 0 & \frac{k_{sF}L_F}{m_{uF}} & \frac{c_{sF}L_F}{m_{uF}} \\ 0 & 0 & 0 & 0 & 0 & 1 & 0 & 0 \\ \frac{k_{sR}}{m_{uR}} & \frac{c_{sR}}{m_{uF}} & 0 & 0 & \frac{-(k_{sR}+k_{tR})}{m_{uR}} & \frac{-c_{sR}}{m_{uR}} & \frac{-k_{sR}L_R}{m_{uR}} & \frac{-c_{sR}L_R}{m_{uR}} \\ 0 & 0 & 0 & 0 & 0 & 0 & 0 & 1 \\ \frac{-k_{sF}L_F+k_{sR}L_R}{I_G} & \frac{-c_{sF}L_F+c_{sR}L_R}{I_G} & \frac{k_{sF}L_F}{I_G} & \frac{c_{sF}L_F}{I_G} & \frac{-k_{sR}L_R}{I_G} & \frac{-c_{sR}L_R}{I_G} & \frac{-(k_{sF}L_F^2+k_{sR}L_R^2)}{I_G} & \frac{-(c_{sF}L_F^2+c_{sR}L_R^2)}{I_G} \end{bmatrix} \begin{bmatrix}x_1\\ x_2\\ x_3\\ x_4\\ x_5\\ x_6\\ x_7\\ x_8\end{bmatrix} + \begin{bmatrix} 0 & 0 \\ 0 & 0 \\ 0 & 0 \\ \frac{k_{tF}}{m_{uF}} & 0 \\ 0 & 0 \\ 0 & \frac{k_{tR}}{m_{uR}} \\ 0 & 0 \\ 0 & 0 \end{bmatrix} \begin{bmatrix}u_1\\ u_2\end{bmatrix}$$

$$\begin{bmatrix}y_1\\ y_2\\ y_3\\ y_4\end{bmatrix} = \begin{bmatrix}1 & 0 & 0 & 0 & 0 & 0 & 0 & 0\\ 0 & 0 & 1 & 0 & 0 & 0 & 0 & 0\\ 0 & 0 & 0 & 0 & 1 & 0 & 0 & 0\\ 0 & 0 & 0 & 0 & 0 & 0 & 1 & 0\end{bmatrix} \begin{bmatrix}x_1\\ x_2\\ x_3\\ x_4\\ x_5\\ x_6\\ x_7\\ x_8\end{bmatrix} + \begin{bmatrix}0 & 0\\ 0 & 0\\ 0 & 0\\ 0 & 0\end{bmatrix} \begin{bmatrix}u_1\\ u_2\end{bmatrix}$$

Matrices

$$A = \begin{bmatrix} 0 & 1 & 0 & 0 & 0 & 0 & 0 & 0 \\ \frac{-(k_{sF}+k_{sR})}{m_c} & \frac{-(c_{sF}+c_{sR})}{m_c} & \frac{k_{sF}}{m_c} & \frac{c_{sF}}{m_c} & \frac{k_{sR}}{m_c} & \frac{c_{sR}}{m_c} & \frac{-k_{sF}L_F+k_{sR}L_R}{m_c} & \frac{-c_{sF}L_F+k_{sR}L_R}{m_c} \\ 0 & 0 & 0 & 1 & 0 & 0 & 0 & 0 \\ \frac{k_{sF}}{m_{uF}} & \frac{c_{sF}}{m_{uF}} & \frac{-(k_{sF}+k_{tF})}{m_{uF}} & \frac{-c_{sF}}{m_{uF}} & 0 & 0 & \frac{k_{sF}L_F}{m_{uF}} & \frac{c_{sF}L_F}{m_{uF}} \\ 0 & 0 & 0 & 0 & 0 & 1 & 0 & 0 \\ \frac{k_{sR}}{m_{uR}} & \frac{c_{sR}}{m_{uF}} & 0 & 0 & \frac{-(k_{sR}+k_{tR})}{m_{uR}} & \frac{-c_{sR}}{m_{uR}} & \frac{-k_{sR}L_R}{m_{uR}} & \frac{-c_{sR}L_R}{m_{uR}} \\ 0 & 0 & 0 & 0 & 0 & 0 & 0 & 1 \\ \frac{-k_{sF}L_F+k_{sR}L_R}{I_G} & \frac{-c_{sF}L_F+c_{sR}L_R}{I_G} & \frac{k_{sF}L_F}{I_G} & \frac{c_{sF}L_F}{I_G} & \frac{-k_{sR}L_R}{I_G} & \frac{-c_{sR}L_R}{I_G} & \frac{-(k_{sF}L_F^2+k_{sR}L_R^2)}{I_G} & \frac{-(c_{sF}L_F^2+c_{sR}L_R^2)}{I_G} \end{bmatrix}$$

$$B = \begin{bmatrix} 0 & 0 \\ 0 & 0 \\ 0 & 0 \\ \frac{k_{tF}}{m_{uF}} & 0 \\ 0 & 0 \\ 0 & \frac{k_{tR}}{m_{uR}} \\ 0 & 0 \\ 0 & 0 \end{bmatrix}$$

$$C = \begin{bmatrix} 1 & 0 & 0 & 0 & 0 & 0 & 0 & 0 \\ 0 & 0 & 1 & 0 & 0 & 0 & 0 & 0 \\ 0 & 0 & 0 & 0 & 1 & 0 & 0 & 0 \\ 0 & 0 & 0 & 0 & 0 & 0 & 1 & 0 \end{bmatrix}$$

$$D = \begin{bmatrix} 0 & 0 \\ 0 & 0 \\ 0 & 0 \\ 0 & 0 \end{bmatrix}$$

5.6.5 Transfer Functions

Quarter-Car

The following transfer functions were calculated based on the A, B, C, and D matrices specified in the state equations section, and using the equation $H(s) = C(sI - A)^{-1}B + D$. The top transfer function is written regarding the chassis height as the output and the ground height as the input. The bottom transfer function is written regarding the wheel height as the output and the ground height as the input.

$$H_1(s) = \frac{sc_sk_t + k_sk_t}{s^4m_cm_u + s^3(c_sm_c + c_sm_u) + s^2(k_sm_c + k_sm_u + k_tm_c) + sc_sk_t + k_sk_t}$$

$$H_2(s) = \frac{s^2k_tm_c + sc_sk_t + k_s}{s^4m_cm_u + s^3(c_sm_c + c_sm_u) + s^2(k_sm_c + k_sm_u + k_tm_c) + sc_sk_t + k_sk_t}$$

Half-Car

The half-car transfer functions were computed using MATLAB, but they are too large to reasonably be displayed in this report.

5.6.6 Controllability

Quarter-Car

The controllability of the quarter-car system was quantified by constructing the P-matrix and observing its rank. The reduced row echelon form (RREF) of the P-matrix was found using MATLAB. The P-matrix, the RREF of P, and its rank are shown below. Two entries to the P-matrix are not shown because they are too large to fit on this page.

$$n = 4$$

$$P = \begin{bmatrix} 0 & 0 & \frac{k_t c_s}{m_c m_u} & \frac{k_t[k_s m_c m_u - c_s^2(m_c + m_u)]}{m_c^2 m_u^2} \\ 0 & \frac{c_s k_t}{m_c m_u} & \frac{k_t[k_s m_c m_u - c_s^2(m_c + m_u)]}{m_c^2 m_u^2} & . \\ 0 & \frac{k_t}{m_u} & \frac{-c_s k_t}{m_u^2} & \frac{k_t[c_s^2(m_c + m_u) - m_c m_u(k_s + k_t)]}{m_c m_u^3} \\ \frac{k_t}{m_u} & \frac{-c_s k_t}{m_u^2} & \frac{k_t[c_s^2(m_c + m_u) - m_c m_u(k_s + k_t)]}{m_c m_u^3} & . \end{bmatrix}$$

$$RREF(P) = \begin{bmatrix} 1 & 0 & 0 & 0 \\ 0 & 1 & 0 & 0 \\ 0 & 0 & 1 & 0 \\ 0 & 0 & 0 & 1 \end{bmatrix}$$

$$rank(P) = 4 = n$$

As seen in the matrices above, the P-matrix has a rank of 4, which equals the number of rows of the P-matrix. Therefore, the quarter-car system is completely controllable.

Half-Car

The controllability of the half-car system was quantified using the same approach as the quarter-car system. The calculations were too complex to do by hand, so MATLAB was used to compute the P-matrix, its RREF, and its rank. The results are shown below.

$$n = 8$$

$$RREF(P) = \begin{bmatrix} 1 & 0 & 0 & 0 & 0 & 0 & 0 & 0 \\ 0 & 1 & 0 & 0 & 0 & 0 & 0 & 0 \\ 0 & 0 & 1 & 0 & 0 & 0 & 0 & 0 \\ 0 & 0 & 0 & 1 & 0 & 0 & 0 & 0 \\ 0 & 0 & 0 & 0 & 1 & 0 & 0 & 0 \\ 0 & 0 & 0 & 0 & 0 & 1 & 0 & 0 \\ 0 & 0 & 0 & 0 & 0 & 0 & 1 & 0 \\ 0 & 0 & 0 & 0 & 0 & 0 & 0 & 1 \end{bmatrix}$$

$$rank(P) = 8 = n$$

As seen in the matrices above, the P-matrix has a rank of 8, which equals the number of rows of the P-matrix. Therefore, the half-car system is completely controllable.

5.6.7 Observability

Quarter-Car

The observability of the quarter-car system was quantified by constructing the Q-matrix for both outputs and observing their ranks. The reduced row echelon form (RREF) of the Q-matrices were found using MATLAB. The RREF of the Q-matrices and their ranks are shown below.

$$n = 4$$

$$RREF(Q1) = RREF(Q2) = \begin{bmatrix} 1 & 0 & 0 & 0 \\ 0 & 1 & 0 & 0 \\ 0 & 0 & 1 & 0 \\ 0 & 0 & 0 & 1 \end{bmatrix}$$

$$rank(Q1) = rank(Q2) = 4 = n$$

As seen in the matrices above, the Q-matrices have ranks of 4, which equal the number of rows of the Q-matrices. Therefore, the quarter-car system is completely observable.

Half-Car

The observability of the half-car system was quantified by constructing the Q-matrix for all four outputs and observing their ranks. The four Q-matrices were constructed using MATLAB. The reduced row echelon form (RREF) of the Q-matrices can hypothetically be found, but MATLAB couldn't calculate them within a reasonable time (the calculations took longer than 6 hours in MATLAB). Therefore, the observability of the half-car system is unknown.

6. Manufacturing Plan

This section discusses the procurement, manufacturing, and assembly of the mechanical, electrical, and software components of the semi-active suspension system.

6.1 Procurement

6.1.1 Mechanical

The mechanical components include the damper, springs, and valve actuator. The damper and valve actuator were provided to the team by Fox Factory. Springs were provided with the dampers, but they are not useful for the Baja's mini-UTV because the spring rates are higher, since the original coilover damper is intended for a full-size UTV. Therefore, new springs were selected to be purchased from F-O-A Off Road Shock Technology. These springs will be purchased online through the Cal Poly Racing Baja SAE team and shipped to campus. The springs were not purchased for this iteration of the project because they were not required for the test bench setup, however they will need to be purchased before the first on-car implementation.

6.1.2 Electronics

All ICs, passive components, microcontrollers, and headers/connectors were purchased through Digikey. Rotary potentiometers were procured as samples through TE Connectivity. All integration materials were procured from the existing inventory of Cal Poly Racing, Baja SAE. All wires/cables, heat shrink, solder, and wire terminals were also be procured from the existing inventory of Cal Poly Racing, Baja SAE.

6.1.3 Software

The STM32L412 Nucleo-32 was acquired from Digikey as described above.

6.2 Manufacturing

6.2.1 Mechanical

Since the damper is too large for the Baja SAE application, it must be modified to fit. To modify the damper, the following procedure will be followed:

1. Remove coilover spring from damper by compressing spring, removing spring retainer at bottom of damper, and pulling off spring.
2. Relieve pressure in external reservoir on damper.
3. Remove bearing cap.
4. Remove shaft assembly from body and drain oil.
5. Remove eyelet from shaft (threaded).
6. Cut 1.5" off the eyelet end of the shaft.
7. Re-die threads.
8. Apply red Loctite to threads and replace eyelet.
9. Cut 1.5" off the open end of the body, debur edges.
10. Refill damper with oil.
11. Replace shaft assembly into body and bleed out air.

12. Hammer bearing cap back into place.
13. Repressurize reservoir to 100 psi with Nitrogen.

6.2.2 Electronics

Part Procurement and Budget

All electronics parts were procured through Digikey, and the Deutsch connectors were procured as samples (no cost) through TE Connectivity. The budget remained the same as what was expressed on the BOM.

Circuit Board

The final prototype design utilizes a breadboard, which has a few advantages over the proposed PCB design. A breadboard was chosen because no soldering is needed, the parts are easily swappable, and the prototype manufacturing can be completed in less than a day. Contrariwise, a breadboard is not a "permanent" solution, making it less than ideal for use on the Baja car. However, this is not an issue because the system is no longer going to be run on the Baja car this year. The advantages of using a breadboard will allow the next SAS team to easily tweak this initial design when bench testing. The final breadboard circuit is shown in the image below.

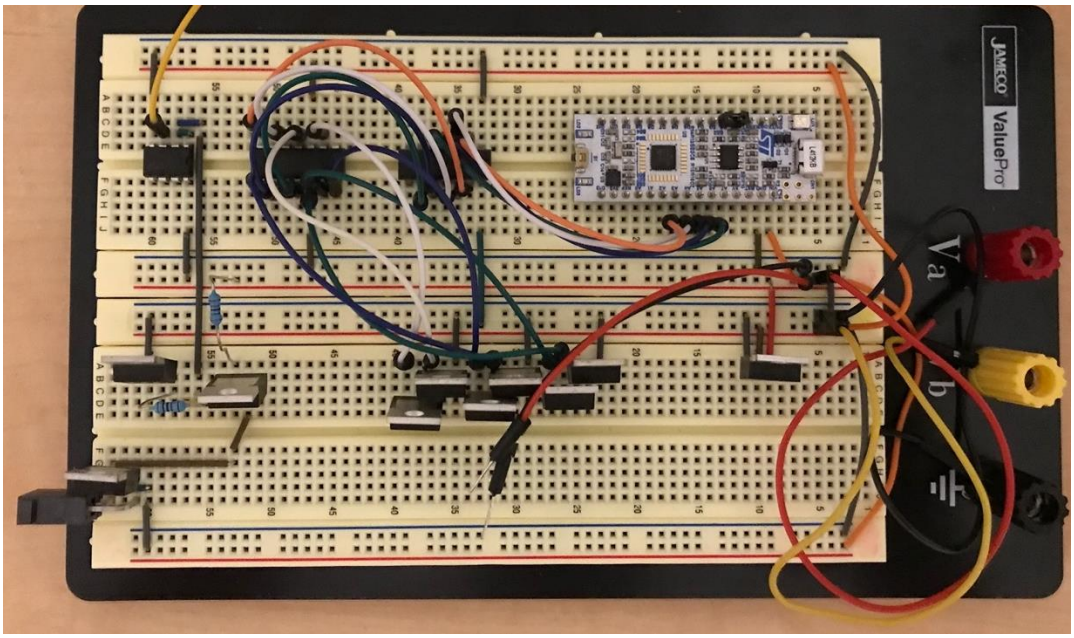

Figure 6.2.1 Electronics Breadboard Circuit Assembly

Circuit Board Enclosure

Due to the transitory nature of a breadboard circuit, the team decided against manufacturing a circuit board enclosure. As the scope of the project changed and the electronics were no longer required to be integrated onto the car this year, a first revision circuit board enclosure was dropped from the scope of the electronics system.

Design Challenges

Circuit temperature testing (section 7.3) has concluded that a large quantity of heat is dissipated through the MOSFETs. Therefore, heat-sensitive components should be placed a safe distance from the MOSFETs. Additionally, it is recommended that a heat sink be bolted on to the MOSFET packaging, and a good amount of airflow should always be present near the MOSFETs.

Future Recommendations

When the circuit is ready to be integrated onto the Baja car, the PCB shall be designed using CAD, and the Gerber file shall be sent to JLCPCB for printing. The PCB shall be printed as two layers in the color white. The PCB components shall be soldered by the SAS team using soldering equipment owned by Cal Poly Racing, Baja SAE. The wiring harness shall be manufactured by the SAS team in the Cal Poly Aero Hangar. The PCB enclosure shall be 3D printed using an SAS team member's 3D printer. The PCB enclosure lid shall be cut out of acrylic using the laser cutter in the Cal Poly machine shop. The integration tabs shall be cut out of 0.125" steel using the Cal Poly water jet. Finally, the integration tabs shall be welded onto the Baja car by a Cal Poly Racing, Baja SAE welder.

6.3 Assembly

6.3.1 Mechanical

Dampers

The dampers will be installed in the rear suspension of the Baja car. They will be assembled in the same location as the passive dampers, with the upper damper mounted on the chassis and the lower damper mounted on the rear A-arm. The electronics will be attached to the valve actuator at the upper end of the damper, closest to the chassis. The wiring will then run along the chassis to the electronics enclosure.

Rotary Potentiometers

The rotary potentiometer will be mounted on a chassis tab near the rear A-arm's mounting points to keep it stationary. The rotary potentiometer has threads near its base, so the potentiometer's output shaft will be inserted through the tab and a washer and nut will be used to secure the potentiometer on the tab. The wiring for the potentiometer will run along the chassis tubes to the electronics enclosure. A lever arm will be used to connect the output shaft of the rotary potentiometer to a fixture on the A-arm. The fixture on the A-arm will be 3D printed and it will clamp over the A-arm tube using a nut and bolt to secure the clamp. The rotary potentiometer mount was not manufactured during this project, since the prototype was used in a test-bench setting. However, future teams can implement this design to integrate the system on-car.

6.3.1 Electronics

All breadboard components were inspected to ensure reliable connections. The electronics breadboard was securely connected to a 12V power supply using a gauge of wire rated for at least 4A. The damper valve was securely connected at one end to the positive rail of the power supply and at the other end to the drain terminal of the MOSFET.

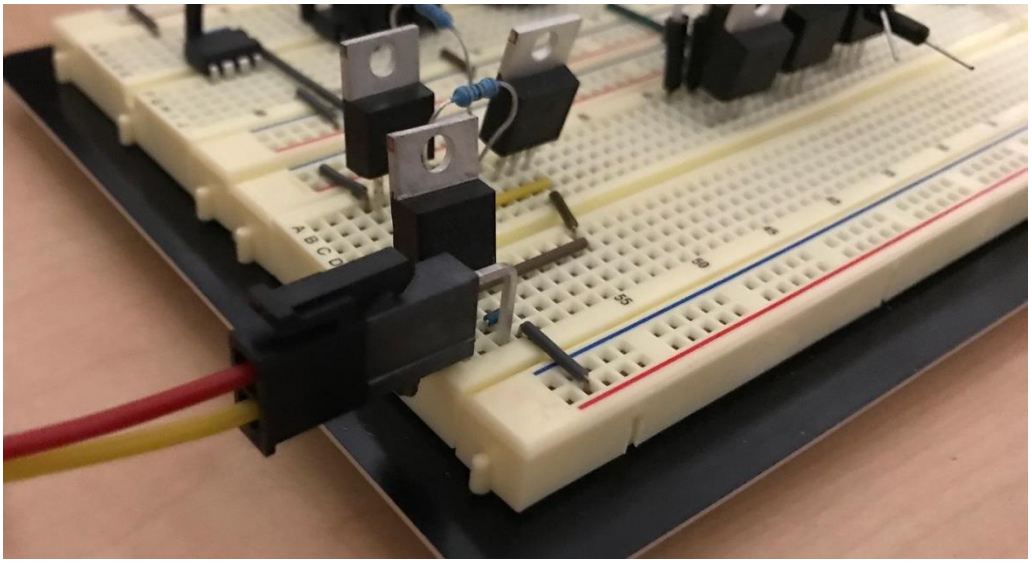

Figure 6.3.1 Electronics Damper Valve Breadboard Interface

7. Design Verification

7.1 Damper control current vs. GPIO voltage

This test was used to measure the accuracy of the damper control circuit. A 12V power supply was used to supply current to the voltage regulator and a damper valve. As a precautionary measure, a high-power resistor was used in place of the damper valve. The resistor had a similar resistance to the damper valve. A waveform generator was used to supply a DC signal to an op-amp input, where the microcontroller would usually supply a signal. Various DC waveforms were passed into the op-amp input, and the output current going through the damper valve was recorded. This test was conducted at home using a power supply, waveform generator, oscilloscope, and SAS quarter-car test circuit. The figure below shows the results of the test.

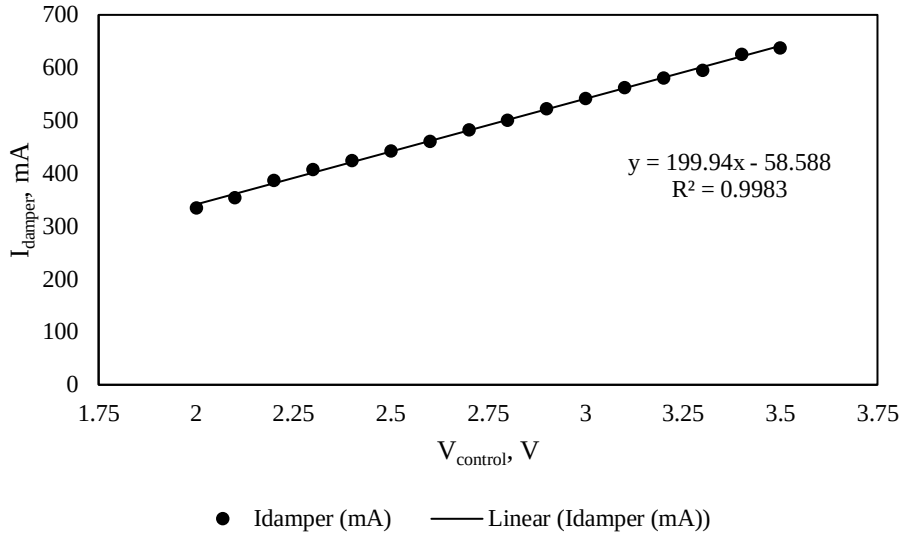

Figure 7.1.1 Damper current (I_{damper}) vs. control voltage ($V_{control}$)

As seen in the graph, the relationship between damper current and control voltage is very linear as shown by its R^2 value of 99.83%.

The resistor used to replace the damper valve has a slightly higher resistance than the damper valve, so the measured current values are slightly lower than the values designed into the circuit. However, the linear relationship can be seen in the graph, so this test was successful.

Additionally, measurements were not taken below a control voltage of 2V because that's where the op-amp hit its rail. This is a design flaw that can easily be corrected by using a rail-to-rail op-amp. This error and a solution will be discussed later in the report.

Further metrics involving this test can be found in Appendix G.

7.2 Damper control current range

This test measured the range of the damper control circuit. A 12V power supply was used to supply current to the voltage regulator and a damper valve. As a precautionary measure, a high-power resistor was used in place of the damper valve. A waveform generator was used to supply a DC signal to an op-amp input, where the microcontroller would usually supply a signal. A precise 3.3V input was introduced to the comparator input, and the output current going through the damper valve was recorded. The test will pass if the output current is about 702mA will a 1% max error. This test was conducted at home using a power supply, waveform generator oscilloscope, and the SAS quarter-car test circuit. The results are shown in the table below.

Table 7.2.1 Damper control current range results

	Measured	**Expected**	
$\boldsymbol{V_{in}\ (V)}$	$\boldsymbol{I_{damper}\ (mA)}$	$\boldsymbol{I_{damper}\ (mA)}$	**Error**
3.3	595	702	15.2%
3.3	588	702	16.2%
3.3	597	702	15.0%
3.3	602	702	14.2%
3.3	601	702	14.4%

As seen in the table above, out of 5 test measurements the average error was around 15%. This is much larger than the allotted 1% error. However, the damper dynamometer test data showed that the damping coefficient doesn't change above a damper current above 600mA. Therefore, a maximum damper current of around 600mA is acceptable. Furthermore, a max damper current of 600mA is more power efficient than a max damper current of 700mA, which reduces the power consumption of the SAS system by around 4.8W at max power ($12V \times 100mA \times 4 = 4.8W$).

The resistor used to replace the damper valve has a slightly higher resistance than the damper valve, so the measured current values are slightly lower than the values designed into the circuit. However, this error is very small (1 to 2 ohms), so the accuracy of this test is reliable.

Further metrics involving this test can be found in Appendix G.

7.3 Circuit Temperature

This test was used to verify that the electronics do not overheat by running the circuit for a single damper at full power. A 12V power supply was used to supply maximum current, 702mA, to the voltage regulator and a single damper valve. As a precautionary measure, a high-power resistor was used in place of the damper valve. Since a constant voltage power supply was used, the control voltage was programmed to supply the damper valve with maximum current constantly as the load changes until the temperature reaches a steady state, which took around 5 minutes. This test was conducted at home using a power supply, waveform generator, SAS quarter-car test circuit, and infrared thermometer. The test will pass if none of the electronics surpass 80˚C (or 176˚F).

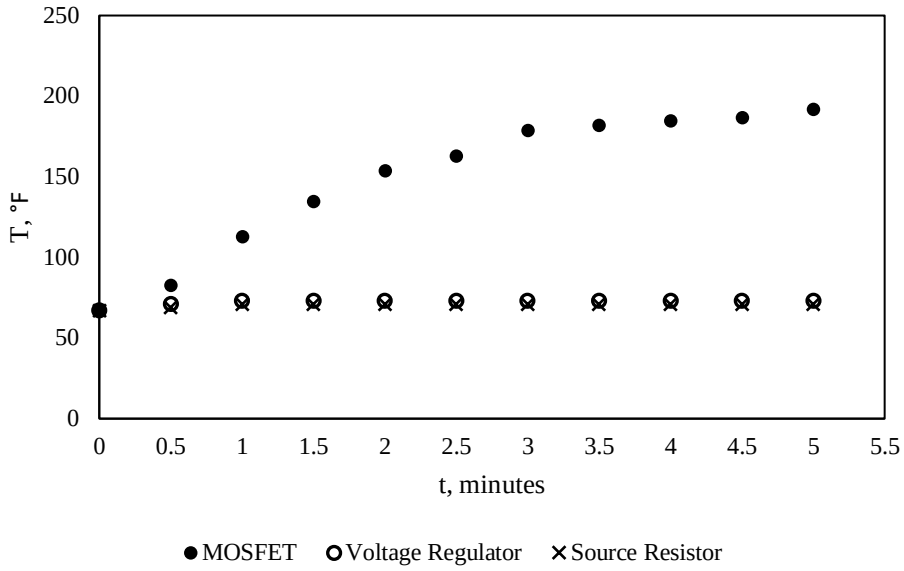

Figure 7.3.1 Component temperatures over time

The temperatures of the three most power dissipating components were measured every 30 seconds. The measured temperatures may have error due to ambient temperature and close timing margins. As expected, the MOSFET proved to rise in temperature far more significantly than the voltage regulator and the source resistor. As seen in the figure above, the MOSFET reached a steady state temperature around 190˚F, which is greater than the maximum temperature of 176˚F to pass the test. To keep the system at a safe temperature, a heat sink will need to be added to all the MOSFETs and sufficient air flow will be needed for proper convection.

Further metrics involving this test can be found in Appendix G.

7.4 Power Consumption

This test was used to calculate the power consumption of the electronics. A 12V power supply was used to supply current to the voltage regulator and a single damper valve. As a precautionary measure, a high-power resistor was used in place of the damper valve. A waveform generator controlled the circuit to run various currents through the damper valve. The voltage and current leaving the power supply were measured and used to calculate the power consumption of the system. This test was conducted at home using a power supply, waveform generator, and SAS quarter-car test circuit. The test will pass if the calculated rate of full-system power consumption does not exceed 11.9Ah over a 4-hour period.

Note: the voltage regulator consumes around 1mA of current without the damper control circuits connected. Therefore, the total system power consumption can be accurately estimated by multiplying the power consumption of a single damper control circuit by four.

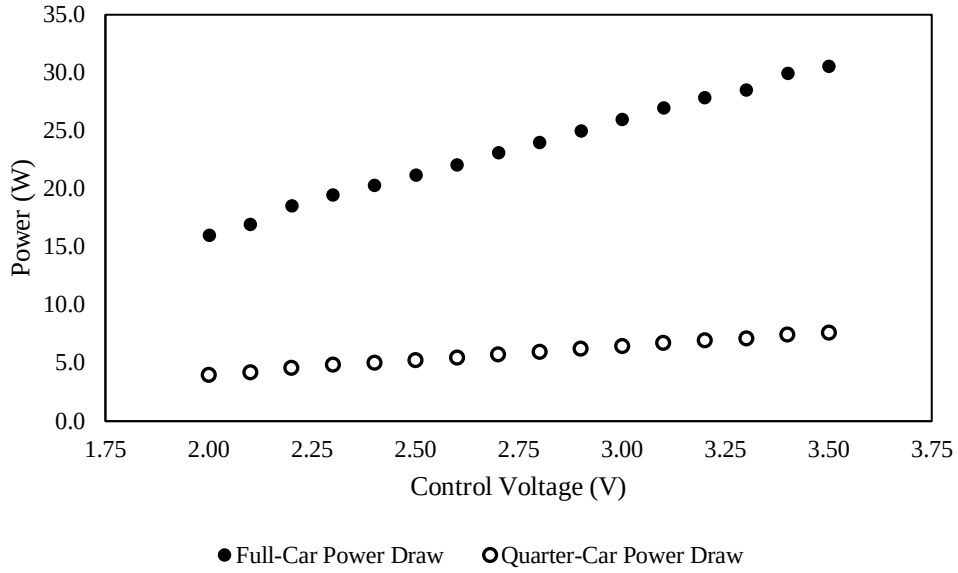

Figure 7.4.1 Power consumption for various control voltages

According to the figure above, the maximum current supplied to the full-car system is approximately 2.55A. This maximum current measurement multiplied by 4 hours gives approximately 10.2Ah, which is under the 11.9Ah limit. Therefore, the power consumption of the system will not completely deplete the battery even if it's run at full load for four hours.

Further metrics involving this test can be found in Appendix G.

7.5 Steady State Response

This test will measure the steady state response of the damping coefficient as a function of the microcontroller output. A 12V power supply will be used to supply current to the voltage regulator and a damper valve. A damper will be placed in a dynamometer, and the dyno will be programmed to run the damper at a constant velocity. This constant velocity must not be too high, so the damper temperature does not vary dramatically. The microcontroller will be programmed to supply the damper with a step input from 0mA to 702mA. The force vs. time graph will be plotted from the damper dyno. Additionally, the voltage vs. time graph will be measured from the microcontroller output using an oscilloscope. The two graphs will be overlayed, and the steady state response time will be measured. The test will pass if the steady state time is under 100ms.

This test will be conducted at Fox Factory using a power supply, oscilloscope, and damper dyno. The test engineer must bring the SAS PCB, microcontroller, and a damper assembly.

This test cannot be completed because the team's timeline did not allow for another trip to the Fox Factory facility. This test will be completed by a future team.

Further metrics involving this test can be found in Appendix G.

7.6 Microcontroller ADC Calibration

Before designing the algorithm, the software commands to the ADC must be validated to ensure that the output signal is correct. This test will measure and calibrate the microcontroller ADC. The microcontroller will be supplied 3.3V using a power supply. An analog GPIO pin will be configured and used to output 500mV to 2.5V in increments of 500mV. The digital input value will be recorded, and the DC analog output value will be measured and recorded. A function will be created to account for any error between the two values. The test will pass once the error becomes less than 10mV.

This test will be conducted at Cal Poly using a power supply and a multimeter. The test engineer must bring the microcontroller. Unfortunately, this test could not be completed in time, because the code to interface with the Nucleo microcontroller was never fully developed. Although using the Nucleo is well-documented, there are not many open-source example code to reference. The team had trouble putting together code to send SPI communication correctly.

Further metrics involving this test can be found in Appendix G.

7.7 Off Car Assembly Time

This test will measure the time it takes to completely install the SAS system on a Baja car. A stopwatch will be used to measure the time it takes a single engineer to install all four dampers, all sensors, the wiring harness, the PCB, and the battery. The test will pass if the time recorded is less than 60 minutes.

This test will be conducted at Cal Poly using a stopwatch and a Baja car. The test engineer must bring the SAS system.

This test could not be conducted because the SAS system was not modified for on-car applications, and therefore could not be test fit and assembled on vehicle. In future projects, this will be a valuable benchmark to determine the feasibility of assembling this electronic control system on the vehicle.

Further metrics involving this test can be found in Appendix G.

7.8 On Car Assembly Time

This test will measure the time it takes to swap out all four SAS dampers with passive dampers. A stopwatch will be used to measure the time it takes a single engineer to remove all four SAS dampers and install passive dampers in their place. This time is important to know in case the SAS dampers need to be replaced with passive dampers during a competition. The test will pass if the time recorded is less than 20 minutes.

This test will be conducted at Cal Poly using a stopwatch and a Baja car. The test engineer must ensure the SAS system is completely installed to begin and have four passive dampers on hand.

This test could not be conducted due to lack of on-car integration since the project focused on a single damper on a test bench setup. This test will be conducted in future projects when four SAS dampers can be installed on-car.

Further metrics involving this test can be found in Appendix G.

8. Project Management

8.1 Design Process

The design process started off with product research, exploring and documenting the various established variable damping strategies used today. To help define the goals and needs of the customer, a growing total of five interviews were organized with industry professionals to learn more about how they have defined their project scopes. They also were able to provide critical feedback on the current approach to the given problem from the customer. Fortunately, the group working on this project are on the Cal Poly Baja SAE team, who are essentially the final customers. This means the project group's understanding of the customer needs is thorough, and that line of communication is continuous. After concluding on the scope of this project, progress will be further made with the Milestones outlined in the next section. These milestones have been added to a Gantt chart, shown in Appendix C, to help the team better manage their time.

8.2 Milestones and Timeline

Table 8.1: Timeline of Milestones and Deliverables

Milestone	Date
Concept Model	05/11/21
Concept Prototype	05/18/21
Preliminary Design Review	05/28/21
Interim Design Review	09/23/21
CAD/Part Selection	10/01/21
Manufacturing Plan Detailed	10/07/21
Critical Design Review	10/28/21
Manufacturing and Test Review	12/01/21
Final Report	03/11/22
Final Prototype Delivered	03/11/22

8.2 Overview of Quarterly Timeline

To give a high-level overview of what has been accomplished and what has yet to be accomplished, this is a quarterly breakdown of how the team has structured the product design process.

8.2.1 Spring 2021

Being the first quarter of senior project, Spring was when the team did their preliminary research and executed interviews to define the team's scope of work. After the scope of work was defined, a series of controlled convergence analysis was done to make the necessary high-level design choices. A functional decomposition was performed, concept prototypes were brainstormed individually, Pugh matrices were created for critical functions, a morphological matrix was made to combine ideas, and a weighted decision matrix ultimately helped to pick the top two final concepts.

8.2.2 Fall 2021

In Fall the team revaluated the project scope and narrowed the project to focus on developing the electronics and control algorithm. The team worked on developing a structural prototype in MATLAB/Simulink to prove the design concept they have developed thus far. Testing on the dampers was done to demonstrate functionality and gather data, while revealing the need for certain modifications needed to make on-car testing possible. Electronics were developed this quarter, including: the current control source, the PCB, and the microcontroller. Implementing the sensor input from the rotary potentiometer is still currently being developed, and the mounting is in the development phase.

With manufacturing plans in place and simulation data to show the benefits of their design, the team plans to start manufacturing the electronics enclosure and mounting tabs.

8.2.3 Winter 2022

Winter is when the team focused on manufacturing the final prototype. The damper was modified (replaced shaft and shim stack) and re-assembled, and the new damper setup was tested at Fox Factory. This allowed the team to achieve the desired damping characteristics despite working with an oversized damper. Additionally, the electronics were assembled during the first 2 weeks of Winter quarter. Then, the team began testing the electronics hardware off-car to ensure the operation specifications are met, as outlined in the Design Verification Plan (DVP), located in Appendix G. The intention was to test the software on a damper dyno at Fox Factory after the electronics hardware was validated, however the team did not validate the software at Fox Factory. The team performed testing to validate the valve performance using a test-bench setup.

The team intended to install the semi-active system onto the Baja car to test the assembly times and ease of use as outlined in the DVP. Additionally, the team intended to begin testing and tuning the system on the 2020 Baja SAE car throughout Spring Quarter. However, the system was proven out on a test-bench and was not implemented on car. Since suspension geometry is likely to change for the 2023 vehicle, the dampers were not modified to fit on the 2022 vehicle and therefore it was not assembled on-car.

8.3 Next Steps

After FDR, the team plans to document all the knowledge and recommendations that have arisen during the first senior project iteration. The team will continue on to advise the next SAS senior project group which will begin in Spring 2022. The team will consult the next senior project team to relay all knowledge and findings so that the second iteration of the project can progress with confidence and achieve on-car status for the 2023 Baja SAE competition.

9. Conclusion & Recommendations

The focus of the Baja SAE SAS senior project is to create a semi-active damper than can continuously vary damping for the Cal Poly Racing Baja SAE racecar. This Final Design

Review Report presents the background research, objective specification, ideation process, concept prototype, design development process, final design concept, manufacturing, design verification, and project management structure to outline the projection of the project and provide documentation of the work completed to this point. Based on the stakeholder's requirements for reaction time, system integration, cost, damping selection range, and further research, a first prototype has been developed. The final design uses an electronic control loop to actuate an off-the-shelf electronic proportioning valve, which continuously adjusts the high-speed compression damping valve. The state of the first prototype is summarized in the following sections along with recommendations for next steps to be completed in the future to further develop a very premature product.

9.1.1 Mechanical Conclusion

Although the mechanical has not been tested on-car, it has been tested on a damper dyno and with a personal power supply and hand dyno. Through these tests it has performed as expected and should only require tuning once adapted to fit on the Baja car. This will undoubtedly bring about other problems to be solved, most likely regarding integration and interfacing. Other than that, the proof of concept is there, and the next team has a solid foundation to start with.

9.1.2 Mechanical Recommendations & Next Steps

Cut Live Valve Dampers
Once the 2023 car's suspension is designed, cut the Live Valve dampers to have the correct extended length and stroke. This will entail cutting the body shorter, making a snap ring groove, and possibly cutting/adding spacers to the shaft.

Verify MATLAB Model
Perform on-car testing to verify that the 7-DOF MATLAB model is tuned reasonably well. This will allow for more reliable testing of algorithms within the software.

9.2.1 Electronics Conclusion

Although the existing design is not suitable to be used at a Baja SAE competition, a few minor adjustments can be made to dramatically improve the performance, reliability, and function of the circuit. Unfortunately for this year's SAS team, since no on-car testing was done, the team was unable to evaluate the hardware design to find the full extent of potential flaws. However, there are clear solutions to each potential problem that will allow next year's SAS team to achieve a "competition-ready" design. Although it is not yet ready to be integrated onto the Baja car, the existing system has proven itself to be a robust, scalable, and reliable bench test circuit.

First, the electronics system scope was tapered back from a full-car integration to a quarter-car bench test circuit. This manifested itself in the form of a breadboard with the ability to control a single damper valve.

9.2.2 Electronics Recommendations & Next Steps

The following recommendations were derived from careful consideration and testing of the existing circuit design.

Replace LM2901N Quad Comparator
The LM2901N does not have a rail-to-rail input, which (as seen in section 7.1) does not allow the control voltage to approach the supply rails. As a result, this means that the damper current cannot drop lower than approximately 330mA (as seen in section 7.1). A proposed solution to this issue would be to replace the LM2901N quad comparator with quad rail-to-rail op-amp. The "rail-to-rail" feature allows for the op-amp output to approach much closer to the supply rails. In return, the damper current could approach much closer to zero.

An alternative approach to this issue would be to redefine the circuit's ground potential. The benefits of this solution are that it might be cheaper and more accurate than using a rail-to-rail op-amp. This would entail the adjustment of the current voltage regulator, and the addition of a voltage regulator to add another supply rail. It is recommended that the new "ground" rail be redefined from 3V to 6V, and a new rail be added about 3.3V above the "ground" rail. This would allow all existing parts to remain the same, but every part's supply voltage would need to be adjusted to meet datasheet specifications. This would also allow the comparator inputs to use their full range because the negative rail will have moved far away from the new "ground" potential.

Account for MOSFET Heat
Add heat sinks and allow for sufficient airflow through PCB housing

Create "Off" State
Open/close MOSFET gates using microcontroller instead of op-amp/comparator output to ensure no current is drawn when MOSFETs are "off". This will require a logic level converter as the MOSFET gate is best driven by the 12V rail, and the logical HIGH output of the STM32 is about 3.3V.

Print Final Design on PCB
The final design of the circuit should be printed on a PCB, which would increase the reliability and save space. A PCB is inherently more reliable than a breadboard because it utilizes soldered connections and protected copper traces. Additionally, as seen in the CAD presented at CDR, the PCB design takes up significantly less room than the breadboard design.

Add Status LEDs
The addition of status LEDs to the final PCB (and even the breadboard) can help with troubleshooting by quickly letting the engineer know which parts of the circuits are connected to power. It is recommended that status LEDs be added to each leg of the damper connections, so that the engineer knows which dampers have a secured connection. It is also recommended that a status LED be added to the 12V and 3.3V power rails so the engineer knows that the correct power is being supplied to the rails.

9.3.1 Software Conclusion

The control algorithm for the damper was simulated in MATLAB as discussed in section 5.2.2. Various algorithm types and road profiles were tested. The simulations yielded little differences when comparing algorithm types and should be developed further and maybe simplified. The main roadblock during the manufacturing stage was programming the Nucleo using the STM32Cube IDE. This halted planned testing that will need to be continued by the team in the future.

9.3.2 Software Recommendations & Next Steps

MATLAB Simulation
Although the MATLAB Simulations were in much need of further development and debugging, they were placed on the backburner after CDR because the team wanted to focus their efforts on building the first prototype. This would be a good first place to do more research into the feasibility of the system. Furthermore, any new control inputs for the SAS system would be simulated here before implemented in the electronics.

Nucleo Testing
Unfortunately since the setup code to communicate to the ADC through the SPI protocol was never built out, the ADC device calibration could not be completed. This would be required to do the full electronics system check for response time and step response behavior. These tests are critical to determine the appropriate application of the semi active suspension system.

Taking User Inputs
The team also wanted to be able to give the microcontroller adjustability during competitions and testing. They did not have the chance, however, to develop a user interface and how exactly, the microcontroller would read these inputs and prompt the user for inputs. This is critical for the usability of the system for calibration, tuning, and racing.

10. References

[1] Buckner, G.D, Schuetze, K. Tand Beno, JH(2000)'Active-vehicle suspension control using intelligent feedback linearization', Proc. of American Control Conference,Chicago,pp.4014-4018.

[2] C. Liu, L. Chen, X. Yang, X. Zhang and Y. Yang, "General Theory of Skyhook Control and its Application to Semi-Active Suspension Control Strategy Design," in IEEE Access, vol. 7, pp. 101552-101560, 2019, doi: 10.1109/ACCESS.2019.2930567.

[3] Carter, AK (1998), “Transient motion control of passive and semi-active damping for vehicle suspensions”, Master these, Virginia Polytechnic institute.

[4] G. Wu, Z. Feng, Gang Zhang and Z. Hou, "Experimental study on response time of magnetorheological damper," 2011 2nd International Conference on Artificial Intelligence, Management Science and Electronic Commerce (AIMSEC), 2011, pp. 3968-3972, doi: 10.1109/AIMSEC.2011.6010142.

[5] Gillespie, T.D. (1992) Fundamentals of Vehicle Dynamics, Society of Automotive Engineers, Warrenale, PA

[6] Grzegorz laski, Michal Maciejewski. Sky-hook and fuzzy logic controller of a semi-active vehicle suspension Poznan University of Technology, Institute of Machines and Motor Vehicles,Prace naukowe politechniki warszawskiej, z. 78 Transport 2011

[7] J. Nandong, "Double-loop control structure for oscillatory systems: Improved PID tuning via multi-scale control scheme," 2015 10th Asian Control Conference (ASCC), 2015, pp. 1-6, doi: 10.1109/ASCC.2015.7244476.

[8] K. E. Majdoub, H. Ouadi, N. Belbounaguia, E. Kheddioui, R. Souhail and O. Ammari, "Optimal Control of Semi-Active Suspension Quarter Car Employing Magnetorheological Damper and Dahl Model," 2018 Renewable Energies, Power Systems & Green Inclusive Economy (REPS-GIE), 2018, pp. 1-6, doi: 10.1109/REPSGIE.2018.8488781.

[9] K. Koyanagi, T. Terada and T. Oshima, "Design of PD controller with Electrorheological fluid damper," SICE Annual Conference 2011, 2011, pp. 2982-2987.

[10] K. Koyanagi, "How does the Time Delay of an ER Fluid's Response Affect Control Performance of Servo-systems?," Proceedings 2007 IEEE International Conference on Robotics and Automation, 2007, pp. 1560-1565, doi: 10.1109/ROBOT.2007.363546.

[11] Karnopp, D.C, Crosby, M.J and Harwood, R.A(1974), Vibration control using semi-active force generators', Journal of Engineering for Industry, VoI.96, No.2, pp 618-626.

[12] Kumbhar, Nilesh & Patil, Satyajit. (2014). A study on properties and selection criteria for magneto-rheological (MR) fluid components. International Journal of ChemTech Research. 6. 3303-3306.

[13] M.V.c. Rao* and V. Prahlad A tunable fuzzy logic controller for vehicle- active suspension systems Fuzzy Sets and Systems 85 (1997) II 21.

[14] Motta,D.S., Zampieri, D.E and Pereia, AK.A (2000), Optimization of a vehicle suspension using a semi active damper', XI Congreso e Exposicao Internacionais da Tecnologia da Mobilidade, Outubro 3 a5,Sao Paulo.

[15] N. Maleki-Jirsaraei, B. Ghane-Motlagh, F. Ghane-golmohamadi, R. Ghane-Motlagh and S. Rouhani, "Synthesis and analysis of the properties of ferro-fluids," 2010 International Conference on Nanoscience and Nanotechnology, 2010, pp. 91-93, doi: 10.1109/ICONN.2010.6045188.

[16] R. R. Anand, S. Shrivastava and M. W. Trikande, "Modelling and analysis of skyhook and Fuzzy logic controls in semi-active suspension system," 2015 International Conference on Industrial Instrumentation and Control (ICIC), 2015, pp. 730-734, doi: 10.1109/IIC.2015.7150838.

[17] Vibration Control of Buildings Using Magnetorheological Damper: A New Control Algorithm: Aly Mousaad Aly-journal of Engineering Volume 2013 (2013), Article ID 596078

[18] Wu Ren, Bo Peng, Jiefen Shen, Yang Li, Yi Yu, "Study on Vibration Characteristics and Human Riding Comfort of a Special Equipment Cab", *Journal of Sensors*, vol. 2018, Article ID 7140610, 8 pages, 2018. https://doi.org/10.1155/2018/7140610

[19] Zadeh L.A, Fuzzy sets, Information and Control, 8: 338-353, 1965

[20] ISO 2631-5:2018, “Mechanical vibration and shock — Evaluation of human exposure to whole-body vibration — Part 5: Method for evaluation of vibration containing multiple shocks”

[21] Fast-Acting Automated Electronic Suspension System: Live Valve, FOX Factory, Inc. 2021. https://www.ridefox.com/content.php?c=livevalve-bike

[22] Fox 2.5 DSC Adjuster – Fits All Brands, AccuTune Products, 2021. https://accutuneoffroad.com/product/fox-racing-shocks-dsc-adjuster-all-brands/

11. Appendices

11.1 Appendix A: Patents

Table 11.1: Patents

Patent Name	Patent Number	Key Characteristics
Magnetorheological fluid damper	US20050087409A1	Uses MR fluid and an electromagnet to create a magnetic field
Adjustable dampers using electrorheological fluids	EP0581476A1	Uses ER fluid and an external power source to create an electric field
Dual live valve shock	20210088100	Changes valving to vary damping, changes both compression and rebound
Electronically adjustable damper and system	US20130328277A1	Uses independent, electronic, remotely controlled valves
High bandwidth control of magnetic ride control system	US8055408B2	Uses MR fluid and a flux command signal to actuate damper force

11.2 Appendix B: QFD House of Quality

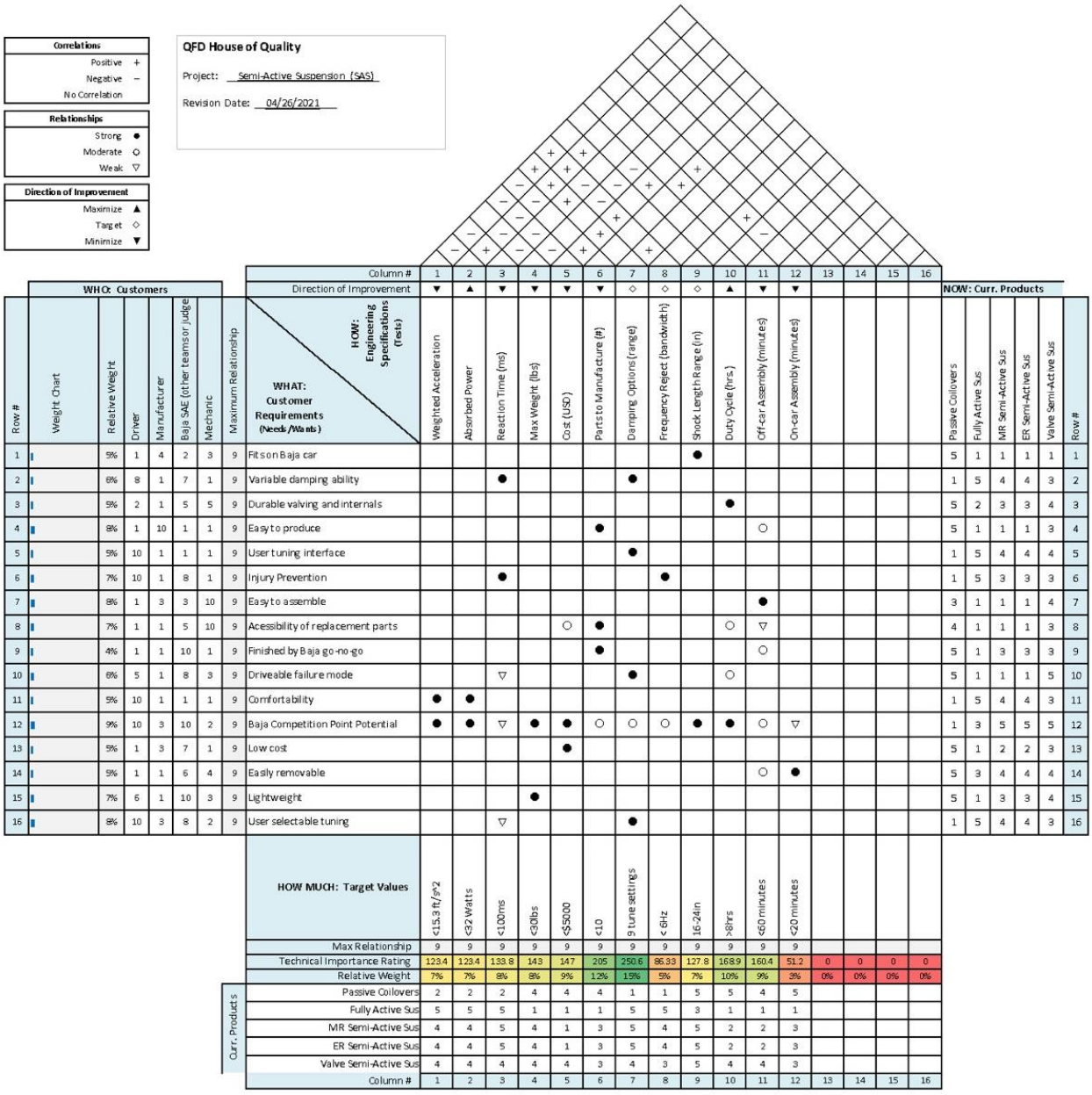

Correlations	
Positive	+
Negative	–
No Correlation	

Relationships	
Strong	●
Moderate	○
Weak	▽

Direction of Improvement	
Maximize	▲
Target	◇
Minimize	▼

QFD House of Quality

Project: Semi-Active Suspension (SAS)

Revision Date: 04/26/2021

		WHO: Customers							HOW: Engineering Specifications (Tests)														NOW: Curr. Products					
	Column #								1	2	3	4	5	6	7	8	9	10	11	12	13	14	15	16					
	Direction of Improvement								▼	▲	▼	▼	▼	▼	◇	◇	◇	▲	▼	▼									
Row #	Weight Chart	Relative Weight	Driver	Manufacturer	Baja SAE (other teams or judge	Mechanic	Maximum Relationship	WHAT: Customer Requirements (Needs/Wants)	Weighted Acceleration	Absorbed Power	Reaction Time (ms)	Max Weight (lbs)	Cost (USD)	Parts to Manufacture (#)	Damping Options (range)	Frequency Reject (bandwidth)	Shock Length Range (in)	Duty Cycle (hrs.)	Off-car Assembly (minutes)	On-car Assembly (minutes)					Passive Coilovers	Fully Active Sus	MR Semi-Active Sus	ER Semi-Active Sus	Valve Semi-Active Sus	Row #
1		5%	1	4	2	3	9	Fits on Baja car									●								5	1	1	1	1	1
2		6%	8	1	7	1	9	Variable damping ability			●				●										1	5	4	4	3	2
3		5%	2	1	5	5	9	Durable valving and internals										●							5	2	3	3	4	3
4		8%	1	10	1	1	9	Easy to produce						●					○						5	1	1	1	3	4
5		5%	10	1	1	1	9	User tuning interface							●										1	5	4	4	4	5
6		7%	10	1	8	1	9	Injury Prevention			●					●									1	5	3	3	3	6
7		8%	1	3	3	10	9	Easy to assemble											●						3	1	1	1	4	7
8		7%	1	1	5	10	9	Acessibility of replacement parts					○	●				○	▽						4	1	1	1	3	8
9		4%	1	1	10	1	9	Finished by Baja go-no-go						●					○						5	1	3	3	3	9
10		6%	5	1	8	3	9	Driveable failure mode			▽				●			○							5	1	1	1	5	10
11		5%	10	1	1	1	9	Comfortability	●	●															1	5	4	4	3	11
12		9%	10	3	10	2	9	Baja Competition Point Potential	●	●	▽	●	●	○	○	○	●	●	○	▽					1	3	5	5	5	12
13		5%	1	3	7	1	9	Low cost					●												5	1	2	2	3	13
14		5%	1	1	6	4	9	Easily removable											○	●					5	3	4	4	4	14
15		7%	6	1	10	3	9	Lightweight				●													5	1	3	3	4	15
16		8%	10	3	8	2	9	User selectable tuning			▽				●										1	5	4	4	3	16
								HOW MUCH: Target Values	<15.3 ft/s^2	<32 Watts	<100ms	<30lbs	<$5000	<10	9 tune settings	< 6Hz	16-24in	>8hrs	<60 minutes	<20 minutes									
								Max Relationship	9	9	9	9	9	9	9	9	9	9	9	9									
								Technical Importance Rating	123.4	123.4	133.8	143	147	205	250.6	86.33	127.8	168.9	160.4	51.2	0	0	0	0					
								Relative Weight	7%	7%	8%	8%	9%	12%	15%	5%	7%	10%	9%	3%	0%	0%	0%	0%					
Curr. Products								Passive Coilovers	2	2	2	4	4	4	1	1	5	5	4	5									
								Fully Active Sus	5	5	5	1	1	1	5	5	3	1	1	1									
								MR Semi-Active Sus	4	4	5	4	1	3	5	4	5	2	2	3									
								ER Semi-Active Sus	4	4	5	4	1	3	5	4	5	2	2	3									
								Valve Semi-Active Sus	4	4	4	4	4	3	4	3	5	4	4	3									
								Column #	1	2	3	4	5	6	7	8	9	10	11	12	13	14	15	16					

11.3 Appendix C: Gantt Chart

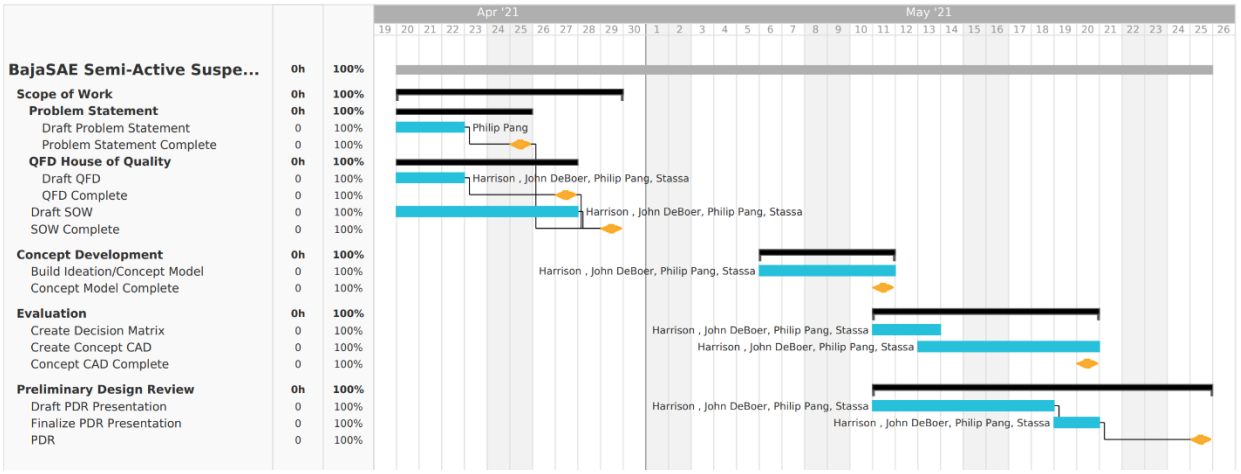

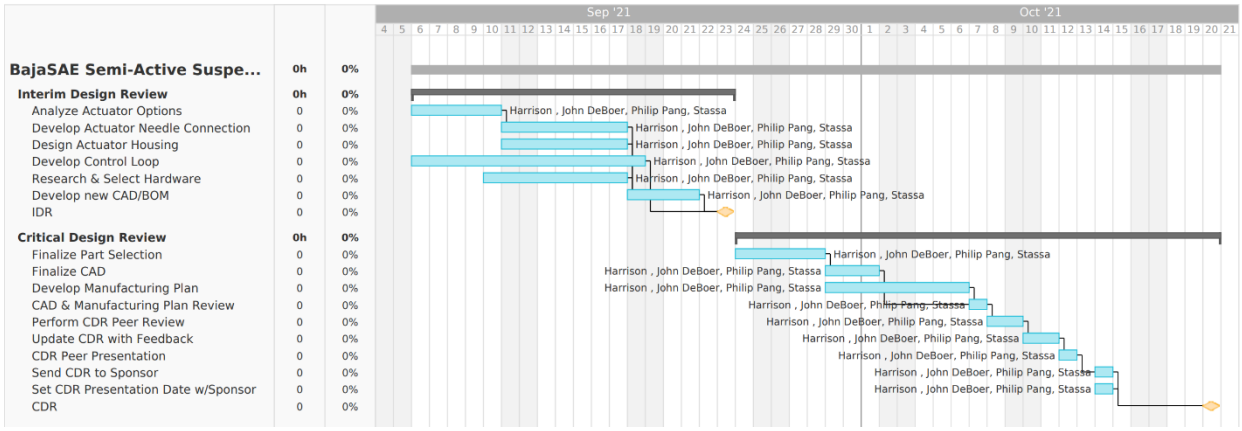

11.4 Appendix D: Design Hazard Checklist

DESIGN HAZARD CHECKLIST

Team: BAJA SAE Semi-Active Suspension Faculty Coach: John Fabijanic

Y	N	
☐	☑	1. Will any part of the design create hazardous revolving, reciprocating, running, shearing, punching, pressing, squeezing, drawing, cutting, rolling, mixing or similar action, including pinch points and sheer points?
☑	☐	2. Can any part of the design undergo high accelerations/decelerations?
☐	☑	3. Will the system have any large moving masses or large forces?
☐	☑	4. Will the system produce a projectile?
☐	☑	5. Would it be possible for the system to fall under gravity creating injury?
☐	☑	6. Will a user be exposed to overhanging weights as part of the design?
☐	☑	7. Will the system have any sharp edges?
☐	☑	8. Will you have any non-grounded electrical systems?
☐	☑	9. Will there be any large batteries or electrical voltage (above 40 V) in the system?
☑	☐	10. Will there be any stored energy in the system such as batteries, flywheels, hanging weights or pressurized fluids?
☐	☑	11. Will there be any explosive or flammable liquids, gases, or dust fuel as part of the system?
☐	☑	12. Will the user of the design be required to exert any abnormal effort or physical posture during the use of the design?
☐	☑	13. Will there be any materials known to be hazardous to humans involved in either the design or the manufacturing of the design?
☐	☑	14. Could the system generate high levels of noise?
☐	☑	15. Will the device/system be exposed to extreme environmental conditions such as fog, humidity, cold, high temperatures, etc.?
☐	☑	16. Is it possible for the system to be used in an unsafe manner?
☐	☑	17. Will there be any other potential hazards not listed above? If yes, please explain on reverse.

For any "Y" responses, complete a row in your Design Hazard Plan including (a) a description of the hazard, (b) a list of corrective actions to be taken, and (c) the date you plan to complete the actions.

11.5 Appendix E: Indented Bill of Materials (iBOM)

Baja SAE Semi-Active Suspension

Indented Bill of Material (iBOM)

Assy Level	Part Number	Descriptive Part Name	Qty	Mat'l Cost	Production Cost	Total Cost	Part Source	More Info
		Lvl0 *Lvl1* *Lvl2* *Lvl3* *Lvl4*						
0	100000	Final Assy						
1	110000	PCB Assembly						
2	111000	Components						
3	111100	NUCLEO-32 STM32L412KB EVAL BRD	1	$ 10.99	$ -	$ 10.99	Digikey	item NUCLEO-L412KB
3	111200	IC QUAD DIFF COMP 14-DIP	1	$ 0.64	$ -	$ 0.64	Digikey	item LM2901N
3	111300	MOSFET N-CH 40V 200A TO220-3	4	$ 2.47	$ -	$ 9.88	Digikey	item CSD18510KCS
3	111400	RES 4.7 OHM 5% 35W TO220	4	$ 3.86	$ -	$ 15.44	Digikey	item TR35JBL4R70
3	111500	RES 10K OHM 1% 1/4W AXIAL	4	$ 0.10	$ -	$ 0.40	Digikey	item RNF14FTD10K0CT-ND
3	111600	RES 1K OHM 1% 1/4W AXIAL	4	$ 0.07	$ -	$ 0.26	Digikey	item CF14JT1K00
3	111700	IC REG LINEAR 3.3V 1.5A TO220-3	1	$ 2.38	$ -	$ 2.38	Digikey	item LM1086CT-3.3/NOPB-ND
2	112000	Board Assembly						
3	112100	Board	5	$ -	$ 0.40	$ 2.00	JLCPCB	
3	112200	2-Pin MOLEX HEADER	1	$ 0.68	$ -	$ 0.68	Digikey	item 0050362457
3	112300	4-Pin MOLEX HEADER	2	$ 0.97	$ -	$ 1.94	Digikey	item 0469990014
3	112400	6-Pin MOLEX HEADER	1	$ 1.26	$ -	$ 1.26	Digikey	item 0050362462
3	112500	2-Pin MOLEX RCPT	1	$ 0.38	$ -	$ 0.38	Digikey	item 0039013025
3	112600	4-Pin MOLEX RCPT	2	$ 0.46	$ -	$ 0.92	Digikey	item 0039013045
3	112700	6-Pin MOLEX RCPT	1	$ 0.47	$ -	$ 0.47	Digikey	item 0039013065
2	113000	Integration				$ -		
3	113100	Mounting Tab	2	$ -	$ -	$ -	CPR Baja	0.125" steel
3	113200	ABS Fillament	1	$ -	$ -	$ -	CPR Baja	
3	113300	M6 Bolt	2	$ -	$ -	$ -	Fastenal	sponsored
3	113400	M6 Nut	2	$ -	$ -	$ -	Fastenal	sponsored
3	113500	M3 Wing Bolt	4	$ -	$ -	$ -	Fastenal	sponsored
3	113600	M2 Bolt	3	$ -	$ -	$ -	Fastenal	sponsored
1	120000	Potentiometers	4	$ -	$ -	$ -	TE	sponsored
1	130000	Wiring Harness				$ -		
2	131000	18-AWG Wire	1	$ -	$ -	$ -	CPR Baja	
2	132000	24-AWG Wire	1	$ -	$ -	$ -	CPR Baja	
2	133000	PET Cable	1	$ -	$ -	$ -	CPR Baja	
2	134000	3-Pin AMP HEADER	4	$ -	$ -	$ -	CPR Baja	
2	135000	3-Pin AMP RCPT	4	$ -	$ -	$ -	CPR Baja	
2	136000	2-Pin AMP HEADER	5	$ -	$ -	$ -	CPR Baja	
2	137000	2-Pin AMP RCPT	5	$ -	$ -	$ -	CPR Baja	
1	140000	12 Ah Battery	1	$ -	$ -	$ -	CPR Baja	
1	150000	Damper Assembly						
2	151000	Dampers	4	$ -	$ -	$ -	FOX Factory	sponsored
2	152000	Valve Actuator	4	$ -	$ -	$ -	FOX Factory	sponsored
2	153000	Springs	4	$ 60.00	$ -	$ 240.00	F-O-A Off-Road Shock	2.5" ID x 16" Length Springs 75 lbf/in
Total Parts			**84**			**$287.64**		

11.6 Appendix F: Manufacturing Plan

Subsystem	Component	Purchase (P), Modify (M), Build (B)	Raw Materials Needed to make/modify the part (only M & B)	Where/how procured?	Equipment and Operations anticipate using to make the component	Key limitations of this operation places on any parts made from it
Damper Modification	Shock body	M	PT-11 Shock oil	Fox Factory donation	1) Use cold saw to cut shock body to desired length 2) Sand to remove burs and sharp edges	
	New Springs	P	--	F-O-A Off-road Shocks	--	
	Shaft	M	--	Fox Shocks donation	1) Use cold saw to cut shaft to desired length 2) Turn cut end for threads 3) Re-die external threads	Need to keep all edges square
Electronics Hardware	ST Nucleo microcontroller	P	--	Digikey	--	
	PCB	M	PCB substrate	JLC PCB	1) Soldering	
	Integration	B	0.125" steel	Baja	1) Waterjet 2) Welding	
	Wiring harness	B	22/4 cable, 22/2 cable, PET cable, heat shrink	Baja	1) Soldering 2) Wire crimping	
	PCB enclosure	B	ABS Filament, acrylic	Baja	1) 3D printing 2) Laser cutting 3) Wire crimping	
Electronics Software	MATLAB Simulink control loop	B	MATLAB	CalPoly	MATLAB 1) Develop first revision with passive data 2) Update model to reference Live Valve data	
	MATLAB SISOtool tuning	B	MATLAB	CalPoly	MATLAB	
	1/4 car model integration	B	MATLAB	CalPoly	MATLAB	
	Position control algorithm	B	STM32 IDE	STMicroelectronics	STM32 IDE	
	Velocity control algorithm	B	STM32 IDE	STMicroelectronics	STM32 IDE	
	Acceleration control algorithm	B	STM32 IDE	STMicroelectronics	STM32 IDE	
	Live-valve damping profile creator	B	MATLAB	CalPoly	Test Data	
	UI	B	MATLAB	CalPoly	MATLAB	

11.7 Appendix G: Design Verification Plan (DVP)

DVP&R - Design Verification Plan (& Report)

Project:	Baja SAE Semi-Active Suspension (SAS)		Sponsor:	Cal Poly Racing, Baja SAE					Edit Date:	10/19/21
TEST PLAN									**TEST RESULTS**	
Test #	Specification	Test Description	Measurements	Acceptance Criteria	Required Facilities/Equipment	Parts Needed	Responsibility	TIMING Start date	TIMING Finish date	Numerical Results	Notes on Testing
1	Damper control current vs. GPIO voltage	Send wave ranging from 0 to 3.3V into circuit input. Verify damper current proportionally scales to GPIO voltage	1) Current through N-MOS source resistor 2) Input voltage	Damper current vs. GPIO voltage can be closely estimated by the equation of a line	1) Power supply 2) Waveform generator 3) Oscilloscope	1) Electronics hardware PCB 2) Damper valve	John	1/17/21	3/3/22	Documented in section 7.1 of FDR report	A high-power 9.4Ω resistor was used in place of the damper valve as a safety precaution
2	Damper control current range	Send wave ranging from 0 to 3.3V into circuit input. Verify damper current range	1) Current through N-MOS source resistor 2) Input voltage	Damper current ranges from about 0mA to about 702mA	1) Power supply 2) Waveform generator 3) Oscilloscope	1) STM32L412KB 2) Electronics hardware PCB 3) Damper valve	John	1/17/21	3/3/22	Documented in section 7.2 of FDR report	A high-power 9.4Ω resistor was used in place of the damper valve as a safety precaution
3	Circuit temperature	Run a single damper control circuit at max load (702mA to all dampers) for 4 hours to verify components don't overheat	1) Temperature of N-MOS 2) Temperature of N-MOS source resistor	Both temperatures remain under 100˚C	1) Power supply 2) Thermometer	1) STM32L412KB 2) Electronics hardware PCB 3) Damper valve	John	1/17/21	3/4/22	Documented in section 7.3 of FDR report	A high-power 9.4Ω resistor was used in place of the damper valve as a safety precaution
4	Power consumption	Run electronics at max load (702mA to all dampers) to verify worst-case power consumption	1) Power supplied to electronics	Total power consumption remains under 12Ah in 4 hour period	1) Power suppply 2) Wattmeter	1) STM32L412KB 2) Electronics hardware PCB 3) Damper valve	John	1/24/21	3/4/22	Documented in section 7.4 of FDR report	A high-power 9.4Ω resistor was used in place of the damper valve as a safety precaution
5	Steady state response	Run damper on dynomometer set at a constant velocity. Send a step function into damper valve stepping from 0mA to 885mA. Send an inverse step function into damper valve stepping from 885mA to 0mA.	1) Force applied to damper over time 2) Current through damper valve over time 3) Settling time	< 100ms settling time	1) Fox Factory shock dyno 2) Power supply	1) STM32L412KB 2) Electronics hardware PCB 3) Damper assembly	Harrison	1/31/21	N/A	N/A	Incomplete
6	Microcontroller DAC calibration	Output 500mV to 2.5V to DAC in 500mV increments. Measure DC output value. Place offset in software if voltage is different than expected.	1) DAC digital input value 2) DAC analog output value	< 10mV error	1) Power supply 2) Voltmeter	1) STM32L412KB 2) Electronics hardware PCB	Philip	1/17/21	N/A	N/A	Incomplete
7	Off car assembly time	Mount all four dampers, wiring harness, sensors, PCB, and battery. Allow no more than one engineer to be assembling the system at a time.	1) Total time	< 60 minutes	1) Stopwatch	1) STM32L412KB 2) PCB 3) Damper assemblies 4) Wiring harness 5) Sensors 6) Battery 7) Baja car	Stassa	1/31/21	N/A	N/A	Incomplete
8	On car assembly time	Swap all four already mounted SAS dampers with 4 passive dampers. Allow no more than one engineer to be assembling the system at a time.	1) Total time	< 20 minutes	1) Stopwatch	1) SAS damper assemblies 2) Passive damper assemblies 3) Baja car	Stassa	1/24/31	N/A	N/A	Incomplete